APPLICATION OF POWER ELECTRONIC DEVICES ON SMART GRID

by

Abdullahi Bala KUNYA

A thesis submitted to

the Graduate Institute of Sciences and Engineering

of

Meliksah University

in partial fulfillment of the requirements for the degree of

Master of Science

In

Electrical and Electronics Engineering

June 2014

Kayseri, Turkey.

This is to certify that I have read the thesis titled "Application of Power Electronic Devices on Smart Grid" by Abdullahi Bala KUNYA and that in my opinion it is fully adequate, in scope and quality, as a thesis for the degree of Master of Science in Electrical and Computer Engineering, the Graduate Institute of Science and Engineering, Melikşah University.

_____

May 20, 2014   Prof. Dr. Tankut YALÇINÖZ

             Supervisor

 I certify that this thesis satisfies all the requirements as a thesis for the degree of Master of Science.

_____

May 20, 2014   Prof. Dr. Murat UZAM

             Head of Department

Examining Committee Members

Title and Name		Approved
Prof. Dr. Tankut YALÇINÖZ	June 2, 2014	_____
Doç. Dr. Ferhat DALDABAN	June 2, 2014	_____
Doç. Dr. İhsan Ömür BUCAK	June 2, 2014	_____

 It is approved that this thesis has been written in compliance with the formatting rules laid down by the Graduate Institute of Science and Engineering.

_____

       Prof. Dr. M. Halidun KELEŞTEMUR

           Director

June 2014.

APPLICATION OF POWER ELECTRONIC DEVICES ON SMART GRID

Abdullahi Bala KUNYA

M.S. Thesis - Electrical and Electronics Engineering

June 2014

Supervisor: Prof. Dr. Tankut YALÇINÖZ

ABSTRACT

The present power system is confronted with a lot of impediments; ranging from reliability problems, faults and voltage inconsistency among others, which originate from the recent sudden increase in demand of electrical power globally. These problems coupled high quality and reliable electrical power demand from the consumers necessitate the utility companies and research groups to devise some techniques to improve the reliability of the whole power system. Among the approaches developed recently, are the turn-around advanced system improvement regarded as Smart Grid technology. The most renown of these techniques applied to distribution system for its reliability improvement are dynamic voltage restorers, fault locator schemes, fault passage indicators, fault current limiters together with substation, distribution and feeder automation which are mainly achieved through the use of power electronics devices. Among these devices, FACTS devices proved to be the leading team. In this thesis, two of these devices; Distribution Static Synchronous Compensator (D-STATCOM) and Dynamic Voltage Restorer (DVR) are modelled and simulated using PSCAD/EMTDC software. Their ability in restoring power quality when there is fault is tested and comparative analysis is carried out. The thesis is extended to testing these devices' capability in integrating photovoltaic system to a utility grid. The impact of PSS on the devices' respective DC link capacitors and power exchanges (active and reactive) taking place between the devices and the AC system is analyzed. This is due the fact that integrating disperse generation sources is one of the important feature of Smart Grid.

Keywords: Smart Grid, Power Quality, D-STATCOM, DVR, PSS, PSCAD/EMTDC.

AKILLI ŞEBEKESİNDE GÜÇ ELEKTRONİĞİ
CİHAZLARININ UYGULAMASI

Abdullahi Bala KUNYA

Yüksek Lisans Tezi – Elektrik ve Elektronik Mühendisliği

Haziran 2014

Tez Yöneticisi: Prof. Dr. Tankut YALÇINÖZ

ÖZ

Dünya çapında elektrik güç ihtiyacı artmasından dolayı günümüzdeki güç sistemleri birçok problemler karşı karşıyadır; güvenilirlik problemi, kısa devre arızaları ve gerilim uyuşmazlığı gibi problemler bunlardan bazılarıdır. Bu problemlerden dolayı araştırmacılar ve elektrik şirketleri tüketicilerin yüksek kalitede güvenilir elektrik gücü isteklerini karşılamak için kullanılacak yeni teknikler bulmaları gerekmektedir. Son zamanlarda geliştirilen yaklaşımlar arasında ileri sistem düzeltmesi olarak bilinen Akıllı Şebekeler teknolojisi sayılabilir. Dağıtım sistemler için en çok kullanılan güvenilirlik iyileştirme tekniklerden dinamik gerilim düzeltici, arıza arama planları, arıza geçiş göstergesi, akım arıza sınırlayıcıları ile transformatör, dağıtım ve besleyicilerin otomasyonu ki bunlar genellikle güç elektroniği cihazlarının kullanımıyla elde edilir. Bu cihazlardan Esnek AC İletim (FACTS) cihazları en iyi çözüm olduğu ispatlanmıştır. Bu çalışmada cihazlardan ikisi; Dağıtık Statik Senkron Düzenleyici (D-STATCOM) ve Dinamik Gerilim Restoratör (DVR)'ü PSCAD/EMTDC yazılımı kullanarak modellendi ve benzetimi yapıldı. Bunların arıza olması durumunda güç kalitesini geri getirebilme kabiliyetleri test edildi ve bu cihazların karşılaştırmalı analizi gerçekleştirildi. Bu tez, bu cihazların fotovoltaik sistem ile şebekeye bağlanması kabiliyetinin testi ile genişletilmiştir. Cihazlar ve AC sistemi arasındaki aktif ve reaktif güç değişiminin fotovoltaik sisteme etkileri incelenmiştir. Şebekeye dağıtılan üretimi kaynaklarını entegresi Akıllı Şebekelerin önemli özelliklerden biridir.

Anahtar Kelimeler: Akıllı Şebeke, Güç Kalitesi, D-STATCOM, DVR, Fotovoltaik Sistem, PSCAD/EMTDC.

DEDICATION

I dedicate this thesis to my parents for their tireless, indefatigable and earnest support, love, and encouragement they have been offering me since childhood to where and how I am today. My achievements in life wouldn't have been materialized without their prayer, guidance and the philosophy of hardworking they imparted on me.

ACKNOWLEDGEMENT

TABLE OF CONTENTS

LIST OF TABLES

LIST OF FIGURES

FIGURE   **PAGE**

LISTS OF SYMBOLS AND ABBREVIATIONS

SYMBOLS

Δ-	Delta connection
A_{sin}	Amplitude of modulating signal
A_{tri}	Amplitude of carrier signal
C_{dc}	Capacitance of the DC link capacitor
E_s	Sending end voltage
f_{sin}	Frequency of modulating signal
f_{tri}	Frequency of carrier signal
m_a	Amplitude modulation index
m_f	Frequency modulation ratio
n	Coupling Transformer turns ratio
S_{12}	Complex power flow form bus 1 to 2
S_{DVR}	Complex power injection
V_{BUS}	Bus voltage at PCC
V_D	DC link capacitor voltage
V_{dcmax}	Preset upper limit of the DC link capacitor
V_{DVR}	DVR DC link voltage
V_{DVR}	DVR output series injection voltage
V_i	D-STATCOM output voltage
V_R	Receiving end voltage
V_s	Supply bus voltage
V_{VSC}	VSC output voltage
X_L	Transmission line reactance
Y-	Star connection
θ_R	Receiving end phase angle
θ_S	Sending end phase angle

ABBREVIATIONS

AMI	Advanced Metering Infrastructure
DGS	Disperse/ Distributed Generation Sources
DSTATCOM	Distribution Static Synchronous Compensator
DVR	Dynamic Voltage Restorer
EMTDC	Electromagnetic Transients for Direct Current
ETP	European Technology Platform
FACTS	Flexible Alternating Currents Transmission Systems
GTO	Gate Turn-off Thyristor
GUPFC	Generalize Unified Power Flow Controller
HEP	Hydro-Electric Power
HVDC	High Voltage DC
BPL	Broadband over Power Line
IGBT	Insulated-gate Bipolar Junction Transistor
IPFC	Inter-line Unified Power Flow Controller
MOSFET	Metal Oxide Semi-conductor Field-Effect Transistor
MPPT	Maximum Power Point Tracking
PCC	Point of Common Coupling
PSCAD	Power System Computer Aided
PSS	Photovoltaic Solar System
SCADA	Supervisory Control and Data Acquisition
SPWM	Sinusoidal Pulse Width Modulation
SSSC	Static Series Synchronous Compensator
UPFC	Unified Power Flow Controller
VSC	Voltage Source Converter

CHAPTER ONE

INTRODUCTION

1.1 PREAMBLE

Sequel to the sudden boost in technological innovations and rapid hike in the world population, high quality and reliable electrical power (in particular) demand has significantly increased recently which is roughly estimated to double by next decade [1]. This impediment has exert a heavy burden on the present traditional power systems leading to so many power quality problems; voltage inconstancy, frequency fluctuations, poor reliability caused as result of overloading the transmission and distribution lines thereby forcing it to its crucial stability and thermal limits [2]. It is statistically established that about 85 to 90% of these problems initiated from distribution systems [3]. These have made operation and maintenance costs agonizingly high, therefore make it necessary for the electric utilities to devise some measures for improving the system reliability. Among the approaches employed are the installation of lightning arrestors, replacing overhead bare conductors with insulated and underground cables or network expansion (construction of new generating stations, transmission and distribution lines). This is not economical, time consuming and environmentally unfriendly, and suffers authorization problems as not all countries allows some [4-6].

Alternatively, some research groups, utility companies and government agencies have envisioned transforming the existing traditional grid into an efficient, self-controlled, sustainable and reliable power grid termed as Smart Grid [7]. This modernized system is expected to encapsulate information, computational intelligence and two-way cyber-secured communication technologies that allows both the consumers and the suppliers (utility companies) to have control over the behavior of the network at large in an automated style unlike the present one that gives only the suppliers such opportunity.

It is also expected to safely accommodate, in to the grid, Distributed Generation Sources (DGS); both renewables and non-renewables like photovoltaic solar farms, wind turbines, fuel cells and wave generators with aid of two-way power flow, sophisticated controls, advanced electric storage system such flow batteries or flywheels, power electronic devices and grid automation technologies. Smart grid technology responds to changes anywhere in the grid, ranging from power generation, transmission, distribution down to consumption by taking necessary actions automatically and communicates with both the utility company and the customers about the situation. Among the key Smart Grid technologies applied to distribution system for system reliability improvement are dynamic voltage restorers, fault locator schemes, fault passage indicators, substation automation, distribution automation, feeder automation and fault current limiters which are mainly achieved through the use of power electronic devices. [8-12].

For Smart Grid to be fully materialized, fast and reliable controls are necessary especially for power quality control and integrating DGS to the grid. Power electronics under the umbrella of Flexible Alternating Currents Transmission Systems (FACTS) play an important role in such applications [4]. They are the best option as fast-solid-state switching devices driven by modern control algorithms are used, thereby ensuring fast, precise and real-time controls for transient or dynamic stability of the power systems [3, 13]. Among these devices, Distribution Static Synchronous Compensator (DSTATCOM) and Dynamic Voltage Restorer (DVR) play exceptionally important role in reactive power compensation and voltage stability in distribution networks [14-18].

1.2 MOTIVATION

The need to transform the existing electrical power grid in to a smart one, necessitates the evolution of Smart Grid. To actualize this, power electronic devices are of paramount importance especially when it comes to power quality control, frequency control and integration of Distributed Generation sources (DGS). Among these devices, STATCOM and DVR have significant contribution to such applications, hence employed for the research. Their efficiency, fast switching ability, coupled with the most efficient modulation for their control, motivated and encouraged me to carry out the research. Power System Computer Aided Design / Electromagnetic Transient for Direct Current (PSCAD/EMTDC) software is used for all the simulations and testing during the research.

1.3 SCOPE/OBJECTIVE OF THE THESIS

The aim and objective of this thesis is to study various advantages and benefits that can be derived from power electronic devices to improve and transform the existing traditional distribution grid to Smart distribution Grid. The scope of the thesis extends to modelling a smart test distribution network, in PSCAD/EMTDC environment, to ascertain the contribution and effectiveness of these devices in handling two-way power flow, which is one of the essential feature of Smart Grid. This network comprises of distribution generation facilities (Photovoltaic), Custom Power devices (Distribution Static Compensator, D-STATCOM and Dynamic Voltage Restorer, DVR, sensitive loads and some balanced faults. These devices are separately tested to determine how effective they are in improving system power quality with and without a photovoltaic system.

1.4 THESIS ORGANISATION

This report is categorically divided into five chapters. After this first introductory chapter, Chapter 2 gives an overview of some Smart Grid technologies, FACTS devices with their basic classifications and applications. The third chapter presents the modelling and design techniques used to come up with the entire test system. Chapter 4 presents simulations carried out together with the results obtained. While the last chapter concludes the report, makes some recommendations and showcased the future work.

CHAPTER TWO

BACKGROUND

2.1 SMART GRID

Electrical grid is an interconnected network for delivering electricity right from generating stations that produce the electrical power, high-voltage transmission lines that carry the power from distant sources to demand centers, and distribution lines that connect individual customers. Fig. 2.1 shows the main components of an electrical grid.

GENERATION
Electricity is generated at various kinds of power plants by utilities and independent power producers.

TRANSMISSION
Electric transmission is the vital link between power production and power usage. Transmission lines carry electricity at high voltages over long distances from power plants to communities.

SUBSTATION

SUBSTATION

DISTRIBUTION
Electricity from transmission lines is reduced to lower voltages at substations, and distribution companies then bring the power to your home and workplace.

Fig. 2.1: Electrical grid main components [19].

The existing power grid has lots of drawbacks; ranging from infrastructural problems, management, security, operational and maintenance costs and the likes. These necessitate the evolution of Smart Grid to solve these problems [7]. All aspect of the present power system have to be upgraded to come up with the Smart Grid.

"Smart Grid is an efficient, self-controlled, sustainable and reliable electrical power grid that encapsulates information, computational intelligence and two-way cyber-secured communication technologies across the entire grid to enable more dynamic flows of information and power thereby integrating the behaviors and actions of all users connected to it; suppliers (utility companies), consumers and those that do both in an automated style." [10, 11].

The system is the state-of–the-art improvement of the existing power grid, as all aspect of power system have to be improved. Power electronic devices are the leading elements in this transformation especially in distribution networks. Fig. 2.2 shows some components of Smart distribution Grid.
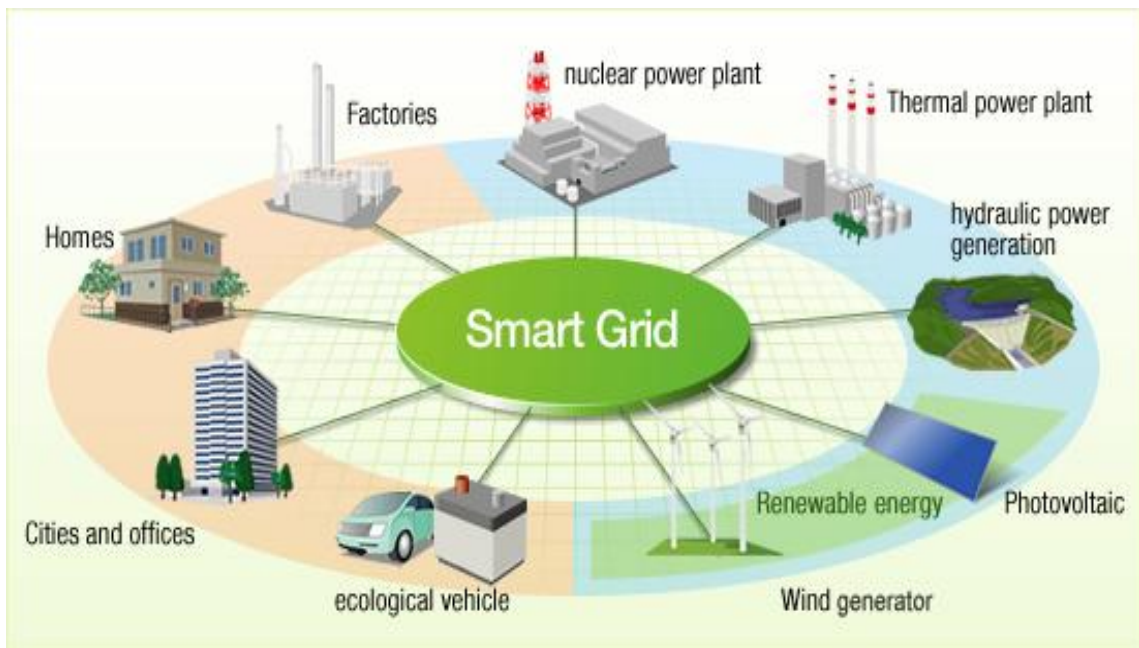
Fig. 2.2: Some components of Smart distribution Grid [20].

European Technology Platform categorically conceptualized the notion of Smart Grid (ETP Smart Grids 2010) on the following factors [10]:

➢ Optimizing grid operation, use and infrastructure
➢ Integrating large intermittent generation
➢ Information and communication technology
➢ Active distribution networks
➢ New market places, users and energy efficiency

While the U.S. Energy Independence and Security Act (2007) emphasized on [11]:

➢ Full cyber-security, smart technologies and appliances
➢ Timely consumer information and control
➢ Standards for communication and interoperability

The present traditional power grid is not fully equipped to accommodate intermittent sources, as it has a single flow path for the power system. Smart Grid technology introduce two-way or multiple channels for power flow and information. This will give consumer the chance to produce electricity through DGS, and supply it to the grid. However, sophisticated controls are needed due power quality distortions. Smart Grid differs from present traditional grid based on many factors as summarized in Table 2.1.

Table 2.1: Difference between existing conventional grid and future Smart Grid [10]

Factors	Existing Conventional Grid	Future Smart Grid
Voltage Control	EM excitation control of generators and manual reactive power control	Achieved through digital power electronic devices control of reactive power
Communication and Power flow	Unidirectional path for Information and power flow	Multidirectional path for Information and power flow
Generation	Centralized	Distributed and robust
Sensing	No or less sensors	Sensors throughout the system.
Monitoring and Troubleshooting	Manually monitored and restored	Computerized monitoring and self-healing
Costs	Expensive operational and maintenance costs	Cheaper due to automation in control and DGs as an alternative for generation
Customer Participation	Less customer choices and participation	Interactively, end-users are involved in the system operations
Environment	Unfriendly because of the emission; heat, burnt carbonized products	Friendly due to the introduction of DGs that gradually decarbonize the electricity

2.1.1 Components of Smart Grid

According to the National Energy Technology Laboratory, the components of Smart Grid are summarized as, but not restricted to [9]:

➢ Advanced system infrastructure; comprising of transmission and distribution networks, power electronics devices (converters, power flow controllers and compensators), plug-in hybrid electric vehicles and distributed generation sources.

➢ Advanced and smart control components; to ensure high power quality, advanced Supervisory Control and Data Acquisition (SCADA) systems, intelligent control systems, long and short term weather forecasting, automation in failure detection and self-healing.

➢ Integrated communications; comprising of digital wireless communication, Broadband over Power Line (BPL) and hybrid power coax.

➢ Sensing and measurement; including advanced protection systems, wireless, intelligent system sensors and Advanced Metering Infrastructure (AMI).

Smart grid, if fully optimized, will not only revolutionize the existing power grid in terms of efficiency, bursting electricity market, consumer participation, monitoring, but will perfectly integrate intermittent generation sources into the grid and can self-heal itself from voltage instability and reactive power problems.
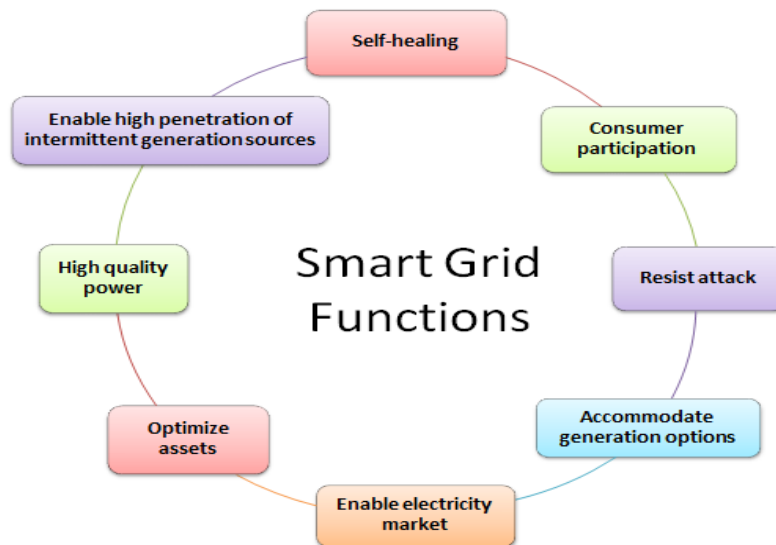
Fig. 2.3: Functions of Smart Grids [20]

To fully establish Smart Grid, power electronic devices, under the umbrella of Flexible Alternating Current Transmission System (FACTS), are very essential especially in power quality improvement, two-way power flow application and integration of alternative energy sources.

This thesis focused on power quality improvement that can be achieved with aid of these devices giving less emphasis on the communication aspect of Smart Grid.

2.1.2 Distributed Generation as an Important Feature of Smart Grid

As part of the provisions of Smart Grid to meet the demand of the consumers with a quality and uniterupted power supply, Distributed Generation facilities are necessary to improve the generation capability and enhance scheduling of the load. It gives consumer the room to sell power to the utility during peak hours and supply himself at the same time, depending on the capacity of the DG. Integrating these systems to the grid causes lots of problem which includes distorting the power quality and causing difficuties in control through voltage and frequency mismatches. However with aid of power electronic converters and compensators, all the these problems can easily be contained. They are grouped based on the type of fuel used [8].

➢ **Renewable Energy Sources;** Photovoltaics, Wind, Tidal or HEP.
➢ **Non-Renewable;** Microturbines, fuel cells, reciprocating engines are based on gas.

Among these DGS, Grid-tied Photovoltaic Solar System (PSS) is choosen and modeled to study its impact to the grid, together with its interaction with FACTS devices in realising Smart Grid.

2.1.2.1 Photovoltaic Solar System

Photovoltaic Solar System (PSS) has wide range of generation capacity ranging from hundreds of MW like in Perovo Ukraine (100MW), Solana Generation Plant, Gila Bend (280MW) and Topaz solar farm (550MW) in USA to small domestic rooftop systems generating few kW [21].

It can be off-grid type; which is not integrated to the grid, or grid-tied system that is connected to the local utility network and can therefore supply power back to the grid through the distribution panel [22].

PSS simply comprises of the solar cells array as the source, DC-DC converter, storage system, DC-AC inverter, filter and distribution panel (in the case of grid-tied) and coupling transformer (typically step-up) as shown in Fig 2.4.
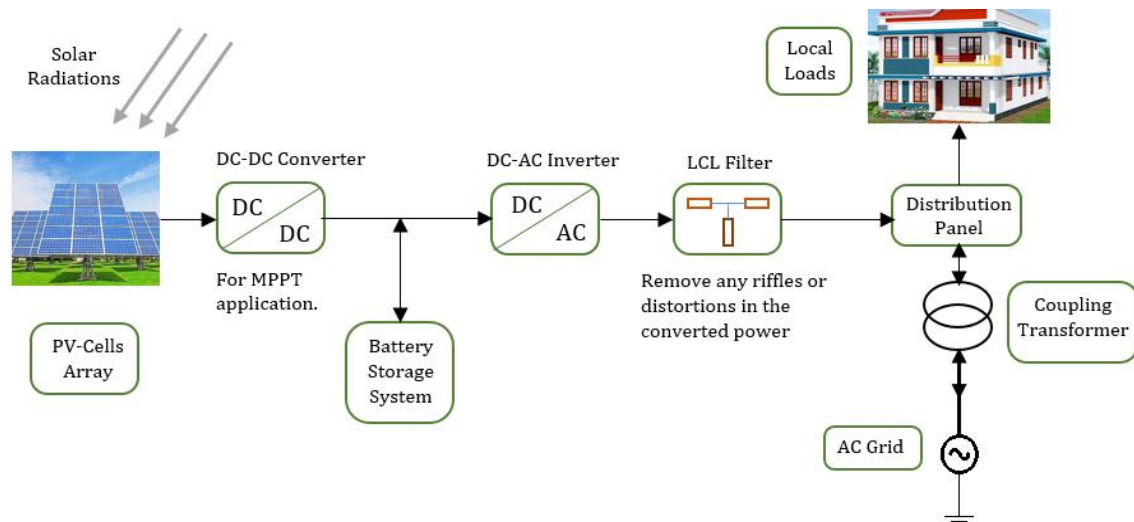
Fig. 2.4: Schematic representation of PSS

The cells receive the solar energy (photons) which energize the charge carriers in the cell thereby generating electron-hole pairs or simply the current. The DC-DC converter employed for Maximum Power Point Tracking (MPPT) maintain the generated power at the MPP. The storage system, mostly comprising of batteries, stores excess energy when the generation exceeds the local demand (in the case of off-grid PSS). This DC voltage is then inverted to AC having same the frequency as the utility [23]. This is achieved with aid of DC-AC inverter after which the riffles and some distortions are removed from the supply through a filter. The coupling transformer steps up the voltage to the grid level and provides a galvanic isolation between the PV and the AC grid [22].

Due to the widely available renewable and sustainable energy source, photovoltaic solar systems have witnessed rapid penetration exponentially in the world market and electrical grid in the last decade.

Fig. 2.5 shows global evolution of PV annual installations from 2000-2012. It can be deduced that European countries patronize PV more than other countries in the world.
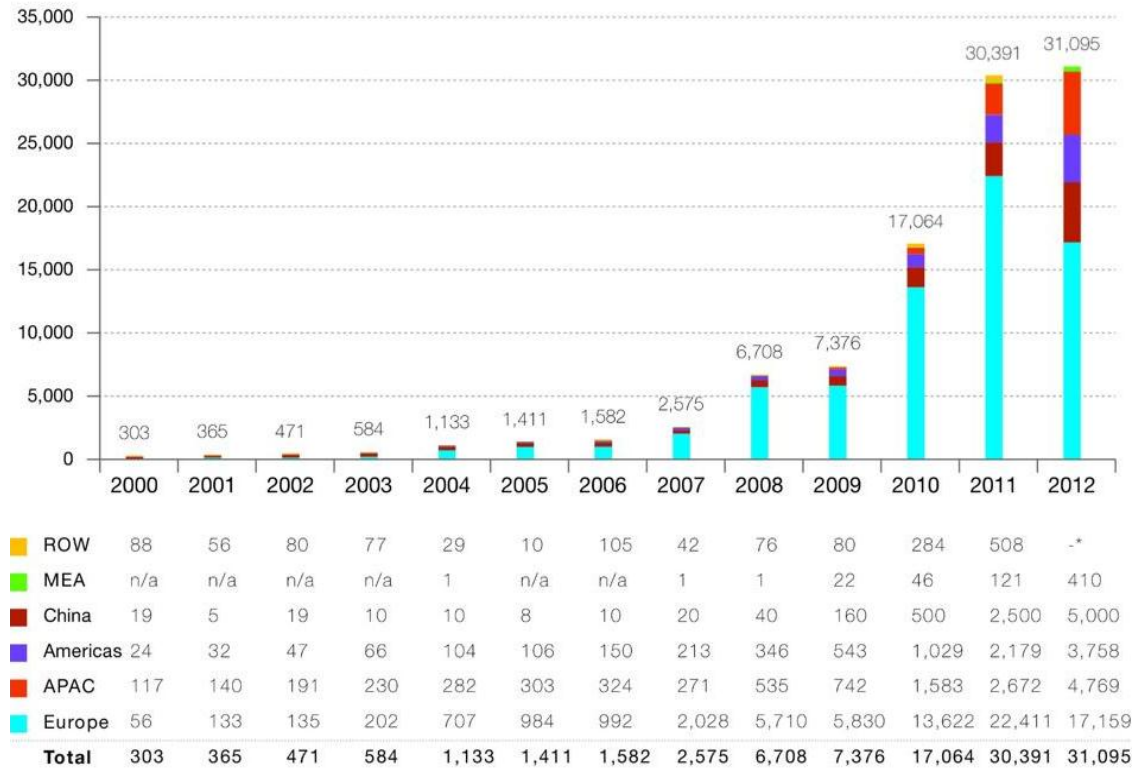
Fig. 2.5: Global evolution of PV annual installations from 2000-2012 [24]

2.2 POWER QUALITY ASPECTS

The fundamental purpose of electrical power system is to efficiently convert energy from one of the naturally existing forms; chemical in natural gas, tidal in waves, potential in waterfall, solar from sun radiation among others, to electrical form and transform it to the consumption centres. While doing so, the system is expected to [2]:

➢ Adjust to continually changing load demand for both active and reactive power
➢ Be environmentally and economically friendly
➢ Meet certain mininum standards in respect to:
  • Voltage Stability
  • Real and reactive power quality
  • Frequency constancy
  • Level of reliability

10

2.2.1 Voltage Stability

Simply defined as the "ability of a power system to maintain steady acceptable voltage levels at all buses in the system under normal operating conditions and after being subjected to a disturbance thereby meeting its reactive power demand" [2]. The main voltage stability problems encountered in the present power system are [25]:

2.2.1.1 Voltage Sag (Dip): Is defined as "a decrease of root mean square (rms) voltage from 0.1 to 0.9 per unit, for a duration of 0.5 cycle to 1 minute". It is believed to be the utmost problem of power quality. It is mainly caused by fault, overloading or starting large induction motors. Fig. 2.6 shows voltage waveform during a balanced sagging. Sagging is similar to brown-out, but the latter takes longer time in the range of minutes or even hours.

2.2.1.2 Voltage Swell: Is defined by IEEE 1159 as "increase of root mean square (rms) voltage from 1.1 to 1.8 per unit, for a duration of 0.5 cycle to 1 minute". It is also referred as "momentary overvoltage", not as common as voltage sagging and mainly caused as result of switching large capacitive loads or de-energizing very large loads. It is depicted in Fig. 2.6.
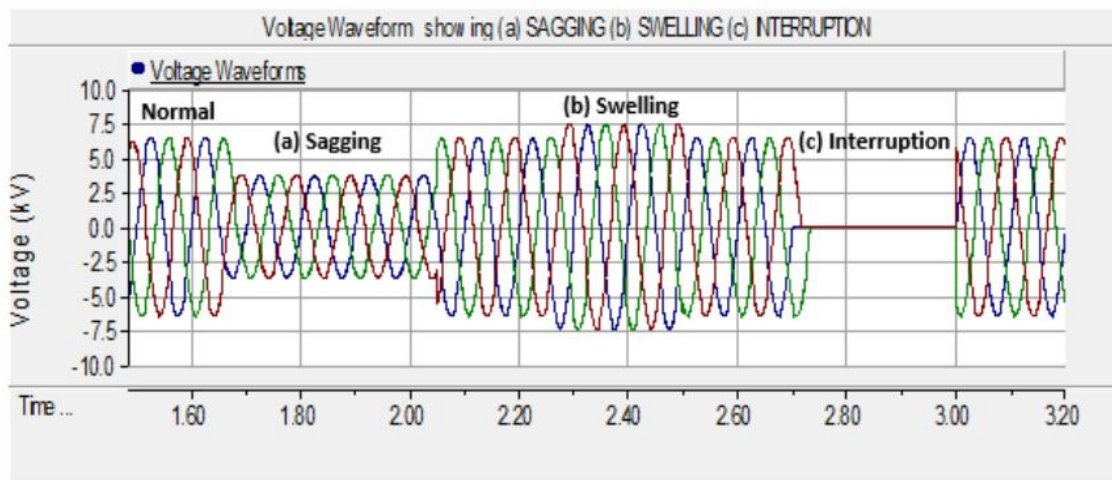
Fig. 2.6: Voltage waveform during balanced swelling, sagging and interruption

2.2.1.3 Voltage Interruption: Is simply the reduction of rms voltage by at least 0.9 p.u within a duration of less than one minute. They are mostly caused by excessive overloading, faults due to accidents, components mal-functions or scheduled downtime (planned). This is depicted in Fig. 2.6.

2.2.1.4 Voltage imbalance (Asymmetry): Is a variation in voltage magnitude or phase angle in a 3-phase system, mainly caused by incorrect distribution of single phase loads. Fig 2.7 shows the voltage waveform with varying magnitudes and phase angle.
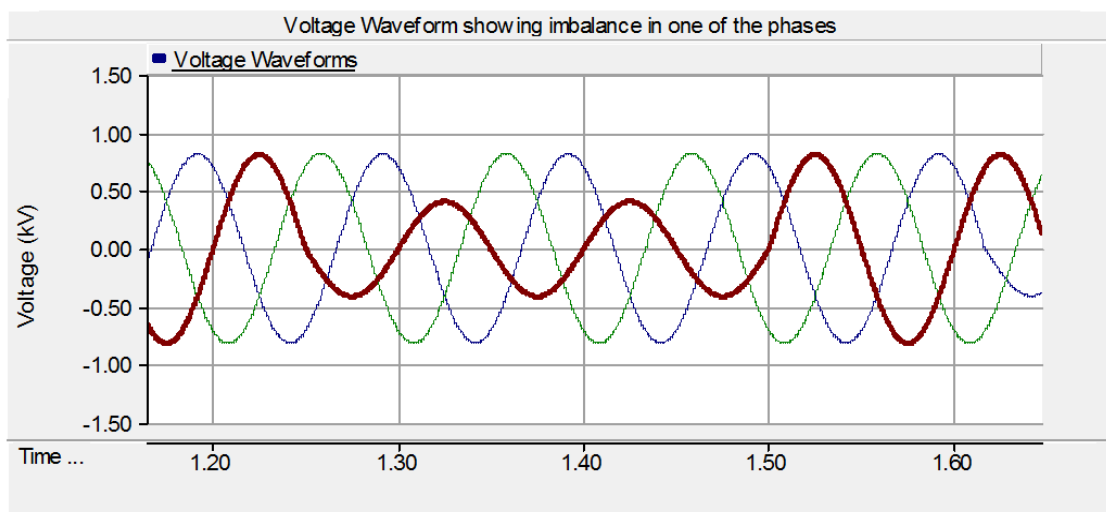
Fig. 2.7: Voltage waveform with varying magnitude in one of the phases

The aforementioned problems and (most likely more) are mostly caused by [2];

➢ Inappropriate locations of FACTS controllers
➢ High reactive power consumption at heavy loads
➢ Occurrence of contingencies
➢ Inverse operation of On-Load Tap-Changer
➢ Locating voltage sources faraway from the load centers
➢ Poor coordination between multiple FACTS controllers
➢ Variation in transmitting reactive power to heavy or sensitive loads

12

2.2.2 Maximum Power Transfer and Control

Referring to Fig. 2.8 that depicts the power flow between two arbitrary buses in a system.
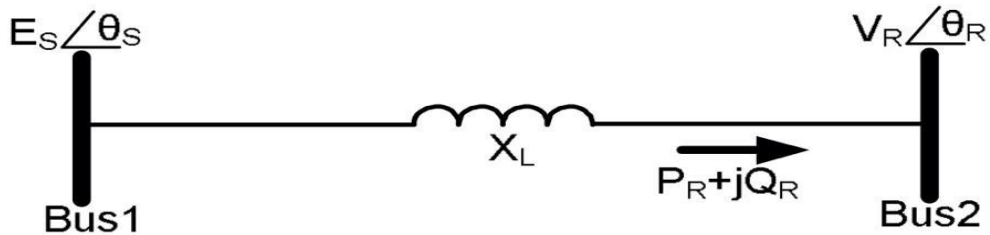
Fig. 2.8: Real and reactive power transfer between two buses [4]

The real power transferred from bus 1 to 2;

$$P_R = \frac{E_S V_R}{X_L} \sin(\theta_S - \theta_R) \tag{2.1}$$

Where E_S, V_R, θ_S and θ_R are the voltages and phases of bus 1 and 2 respectively. X_L is the transmission line reactance having negligible resistance and capacitance. Fig. 2.9 depicts the power-angle characteristic curve, obtained from Equation (2.1) by keeping the $\frac{E_S V_R}{X_L}$ term constant. This shows that the maximum power is transferred at the phase shift of $\frac{\pi}{2}$.
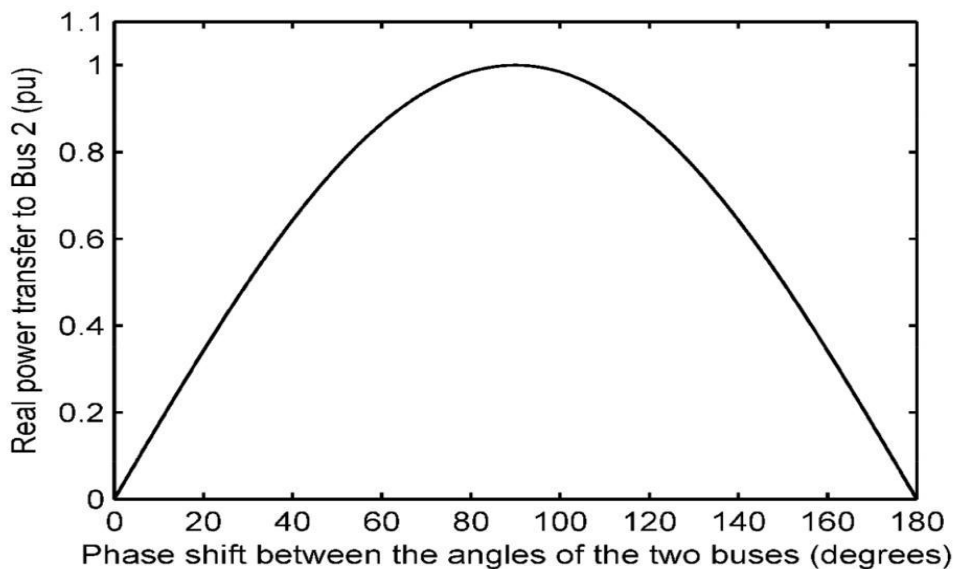
Fig. 2.9: Power-angle curve of a transmission line [4]

The complex power transferred from bus 1 to 2;

$$S_{12} = P_R + jQ_R$$

$$= E_S I^* \tag{2.2}$$

$$I_{12} = \frac{E_S - V_R}{X_L} \tag{2.3}$$

I_{12}, P_R and Q_R are the current and power flowing from bus 1 to 2 respectively.

$$S_{12} = \{|E_S|^2 - |E_S||V_R|\angle (\theta_S - \theta_R)\}(G + jB) \tag{2.4}$$

For a lossless transmission line, the conductance $G \cong 0$. The real part of Equation (2.4) shows the real power received at bus 2, while the imaginary shows the reactive power.

$$P_R = |E_S||V_R|\, B\sin(\theta_S - \theta_R) \tag{2.5}$$

$$Q_R = |E_S|^2 B - B|E_S||V_R|\cos(\theta_S - \theta_R) \tag{2.6}$$

Simplifying for V_R in Equation 2.5 gives the P-V (nose) curve (Equation 2.7) that is used to determine the stability of a system with respect to real power and voltage.

$$|V_R|^2 = \frac{|E_S|^2}{2} - \frac{\beta P_R}{B} \pm \left[\frac{|E_S|^4}{4} - \frac{P_R}{B}\left(\frac{P_R}{B} + \beta|E_S|^2\right)\right]^2 \tag{2.7}$$

Where B is the susceptance of the line and β is the tangent of the power angle. Fig. 2.10 shows the P-V curve at various power factors.
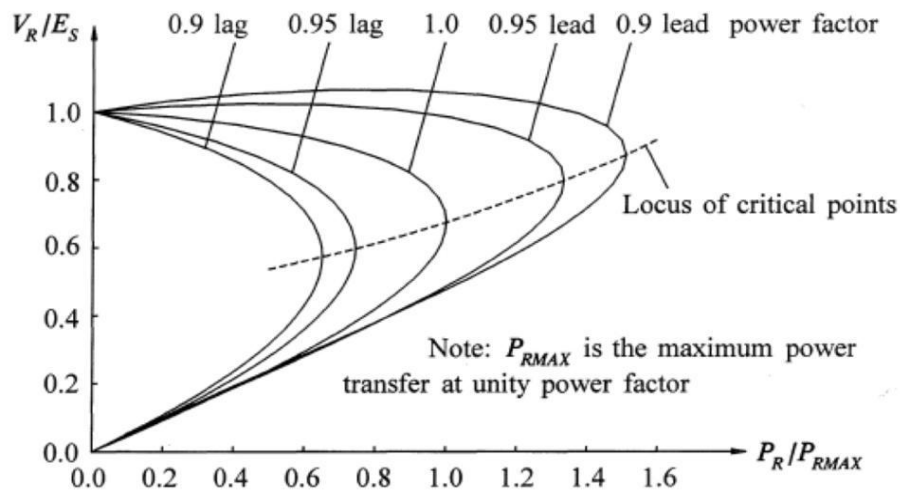
Fig. 2.10: P-V curve at various power factors [4]

The operating points above the dashed lines is in the voltage stable operation and is critically stable if is operating along the locus of critical locus point. While below the

14

critical operating point, the system is unstable which may lead to system breakdown. Fig. 2.11 shows the Q_R-V_R curve at bus 2 obtained from Equation 2.6.
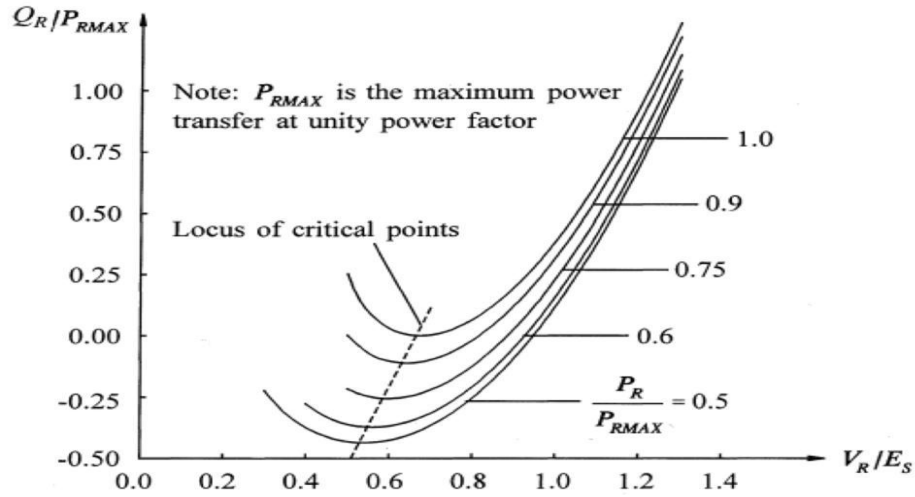
Fig. 2.11: Q-V curve showing the critical stability point [4]

Voltage stability limit is reached at the critical point where the $\frac{dQ_R}{dV_R}$ reaches zero. The system is completely unstable where the gradient of the curve is negative (left of the locus of critical points) and is stable at the right side of the locus. However, stable operation can be achieved at the left side of the locus (unstable region) through the effective use of reactive power compensation techniques with FACTS devices [4].

2.3 OVERVIEW OF FACTS DEVICES

FACTS devices are defined as "*a power electronic based system and other static equipment that provide control of one or more AC transmission system and increase the capacity of power transfer.*" [25].

Due to the complexities of power transmission and distribution networks especially when coupled with DGs, the use of fast switching high-power electronics is inevitable to enhance the system's reliability, robustness and maintainability [4]. This is in addition to providing enabling environment for DGs integration to the grid.

There are so many types of these devices, even though some are modernized to improved their switching capability and power handling capacity. Before installing these devices, three main factors are to be considered [5]:

➢ The type of the device
➢ The (power handling) capacity required
➢ Suitable location to optimize the device performance

2.3.1 Benefits of FACTS Devices for Power Quality

Employing these devices in either distribution or transmission system will effectively [4]:

➢ Optimize system operation by reducing power losses and improving voltage profile
➢ Increase the system's reliability and availability by overcoming problems of dynamic voltage fluctuations; voltage sags and swells.
➢ Enabling the system to fully utilize the existing T and D assets.
➢ Improve the dynamic and transient grid stability and reduction of loop flows.
➢ Correct power quality problems ranging from pf correction, harmonic distortion reduction, phase angle control and limitation of fault currents among others.
➢ Integrate renewable and distributed generation sources to their storage and the grid.

2.3.2 Classification of Power Electronic Devices

Whether employed for distribution system; referred to as custom power devices or in transmission, FACTS devices can be classified based on many factors [4, 13]:

➢ **Configuration or connection style to the network**

Depending on their connection type to the network, FACTS can also be categorized as:

- Series FACTS devices
- Shunt FACTS devices
- Combined Series-Series FACTS devices
- Combined Shunt-Shunt FACTS devices
- Combined Shunt-Series FACTS devices

➢ **Switching properties**

FACTS can also be grouped based on the nature of the semi-conductor devices used:

- First Generation or conventional FACTS devices works like passive elements using impedance or tap changing transformer monitored by a gate controlled Thyristor or Silicon Controlled Rectifier (SCR).
- Second Generation or Converter based FACTS devices using VSC-based control, having the ability to generate active power and exchange reactive power with the system. They have faster response time of about 1-2 cycles.

Tables below summarize these groupings with some application areas of these devices.

Table 2.2: Classification of major FACTS (First Generation) devices [4, 13]

DEVICE	CONNECTION	APPLICATION AREA
First Generation Devices		
Thyristor Control Series Capacitor Compensation (TCSC).	Series	Limitation of fault current, Oscillation damping, sub-synchronous resonance mitigation, voltage stability and Power flow control.
Static VAR Compensator (SVC)	Shunt	Reactive Power (VAR) compensation, Power oscillation damping, voltage stability and control.
Thyristor Controlled Phase Angle Regulator (TCPAR)	Combined Shunt-Series	
Thyristor Controlled Voltage Regulator (TCVR)	Shunt	Muffling of oscillation and transitory, reactive power (VAR) compensation, voltage stability and control, active power (VAR) control.

Table 2.3: Classification of major FACTS (Second Generation) devices [3-6]

Second Generation Devices			
Single Converter	(Distribution) Static Synchronous Compensator (STATCOM)	Shunt	Voltage stability and control, power oscillation damping, reactive power compensation.
	Dynamic Voltage Restorer / Static Series Synchronous Compensator: (DVR/SSSC)	Series	Voltage and power flow control, reactive power compensation, oscillation damping, mitigation of sub synchronous resonance.
Multi-Converter	Unified Power Flow Controller (UPFC)	Combined Shunt-Series	Voltage and power flow control, reactive power compensation, muffling of oscillation, limitation of fault currents.
	Inter-line Power Flow Controller (IPFC)	Combined series-series	Multi-line power flow, voltage control and stability, mitigation of sub-synchronous resonance, reactive power compensation, power oscillation damping.
	Generalized Unified Power Flow Controller (GUPFC)	Combined shunt-series	
	Back-to-back STATCOM	Combined Shunt-Shunt	Real power transfer, reactive power compensation, voltage stability, muffling of oscillation.

2.3.3 Distribution STATCOM (D-STATCOM) Review

D-STATCOM is a VSC based, shunt power electronics device capable of mitigating voltage transients, eliminating line current harmonics as well as reactive power compensation by injecting current into the distribution system thereby exchanging real and reactive power with the system. It is perceived to be the advanced version of SVC, with faster response, modular and requiring less space and have interfacing capability with storage systems [4, 17]. Mostly, it is installed between the supply bus and the sensitive load at point of common coupling (PCC). In its basic configuration, it has a DC

link comprising of an energy storage, Voltage Source Converter (VSC), coupling transformer and controller as shown in Fig 2.12.
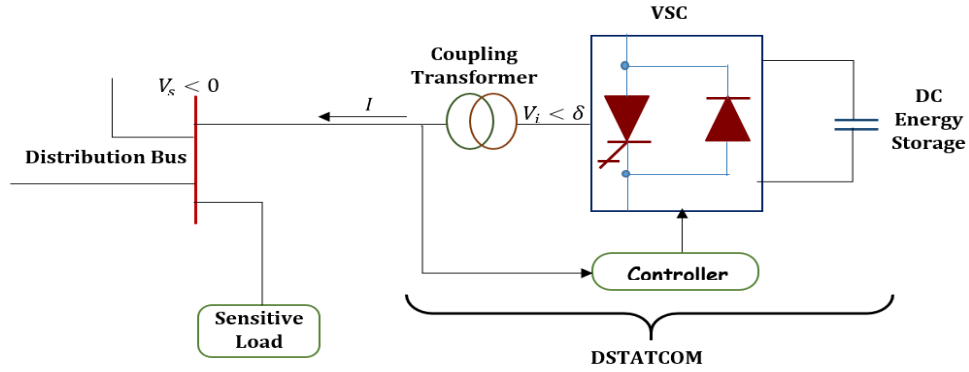
Fig. 2.12: D-STATCOM building block [15]

The coupling transformer in Y-Y configuration, the supply bus voltage, V_s and the DSTATCOM output voltage V_i has, respectively, the following instantaneous values:

$$V_{sa} = \sqrt{2}\, V_s \sin \omega t$$

$$V_{sb} = \sqrt{2}\, V_s \sin(\omega t - 2\pi/3) \tag{2.8}$$

$$V_{sc} = \sqrt{2}\, V_s \sin(\omega t + 2\pi/3)$$

$$V_{ia} = \frac{\sqrt{3}}{2} n m_a V_D \sin(\omega t + \delta)$$

$$V_{ib} = \frac{\sqrt{3}}{2} n m_a V_D \sin(\omega t + \delta - 2\pi/3) \qquad .(2.9)$$

$$V_{ic} = \frac{\sqrt{3}}{2} n m_a V_D \sin(\omega t + \delta + 2\pi/3)$$

V_D, n and m_a are the DC voltage across the capacitor, coupling transformer turns ratio and PWM amplitude modulation ratio respectively. The frequency and the phase angle of the three phase output voltage of the VSC solely depends on the gate pulse pattern [14].

By suitable adjustment of the phase angle and magnitude of STATCOM's output voltage (which proportional to the DC link voltage) and the AC voltage, real and reactive power exchange occurring between the system and the STATCOM at the point of common coupling (PCC) can be controlled as depicted in Equation (2.10 and 2.11).

Real; $$P = \frac{V_{vsc}\, V_{bus}}{X_L} \sin \delta \tag{2.10}$$

Reactive: $Q = \dfrac{V_{bus}^2}{X_L} - \dfrac{V_{vsc}\,V_{bus}}{X_L}\cos\delta$ (2.11)

Where the voltage across the coupling transformer; $V_{bus} = V_{vsc} + V_{load}$ (2.12)

It is therefore operated in both capacitive and inductive mode as shown in Fig. 2.13 [14].

(a) Capacitive Mode

(b) Inductive Mode

(c) Active Power Discharge

(d) Active Power Absorption
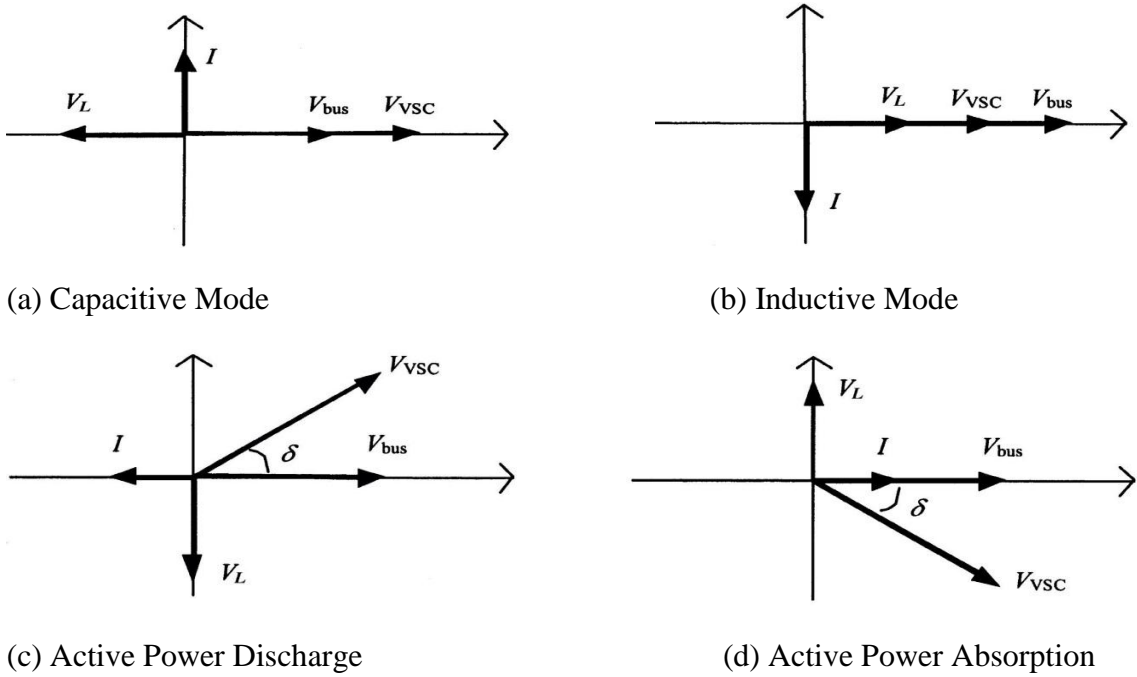
Fig. 2.13: Vector representation of operating modes at fundamental frequency [14]

Table 2.4 summarizes the exchange of power flow path with respect to V_{vsc}, V_{bus} and δ.

TABLE 2.4: Power flow exchange between DSTATCOM and the AC system [14]

Voltage Relation	Power Exchange			Modes/Functions
	DSTATCOM	$\leftrightarrow$	AC SYSTEM	
$|V_{vsc}| > |V_{bus}|$	Q	$\rightarrow$		Capacitive
$|V_{vsc}| < |V_{bus}|$		$\leftarrow$	Q	Inductive
$\delta < 0$	P	$\rightarrow$		Active power absorption.
$\delta > 0$		$\leftarrow$	P	Active power discharge.

20

The VSC (which can be 6- pulse, 12- pulse, 24- pulse or even higher quasi multi-pulse) converts the DC voltage in the DC link into three-phase AC output voltages, which are then coalesced to the network via the reactance of the coupling transformer [4]. PWM-based control scheme generates the switching signals that control the valves of the power electronic device used in the VSC. This is explained in the next section of this chapter.

2.3.4 Dynamic Voltage Restorer (DVR) Review

DVR have similar configuration as DSTATCOM but its coupling transformer is connected in series with the main AC system as shown in Fig 2.14 below. It is commonly used for voltage regulation (as in this thesis), harmonics level suppression and improving the power quality with conventional real and reactive power control [16, 26].

Fig 2.14: DVR building block [15]

The DC energy storage is responsible for energy storage in DC form. Many devices, with different energy efficiencies, can be used as energy storage mechanism. T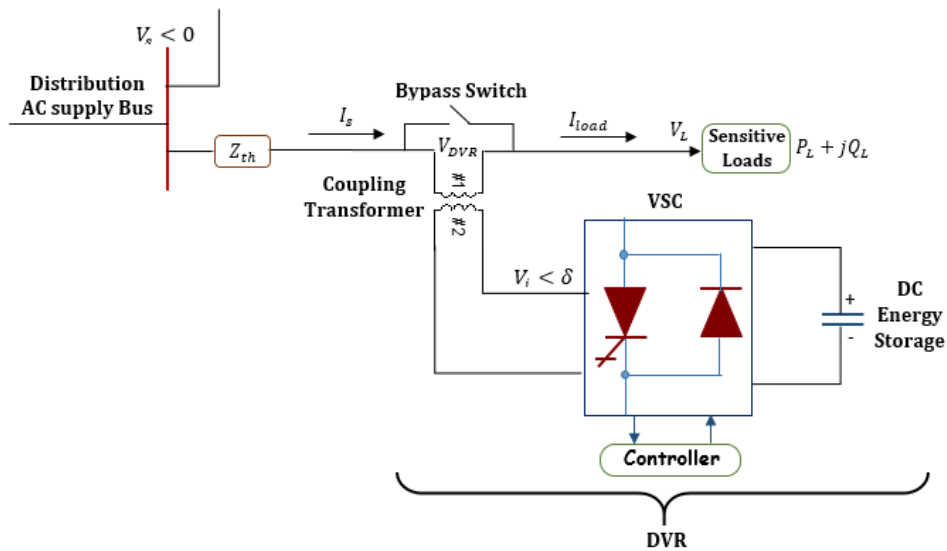hese include Superconducting Magnetic Energy Storage (SMES)-90%, Fly wheel – 80 %, Compressed air – 80% and lead acid batteries – 75 % [27]. These can be grouped as constant DC link voltage systems.

In some applications, the DC link is re-enforced with a fuel cell [28], wind farm, photovoltaic solar system [22], or a hybridized system of these distributed sources. These are referred as variable DC link voltage systems. Certain configuration exist in such a way that the DVR takes its input power from the main grid through a step-down transformer. This eliminate the DC link capacitor application as presented in [16].

Storage capacity and the discharging period are the main factors under consideration in determining the best mechanism. Table 2.5 categorizes the application area of energy storage system with respect to their storage ability and discharging time.

Table 2.5: Energy storage applications based on storage capacity and discharge time [18]

Application	Storage Capacity	Discharge Period
Power grid leveling	11MJ - 201GJ	Few seconds- few Days
Power quality	0.11 - 11MJ	Few seconds
Custom power devices	0.11 - 11MJ	Few cycles

The size of the capacitor and the corresponding DC source depend on the application and power requirement (voltage level) of the system [16, 27].

2.3.4.1 Voltage Sag/Swell calculation

For a balanced loading system, the currents through load 1 and 2 in Fig 2.15 are equal. Faults or connecting heavy load to one feeder will alter the system's symmetry.
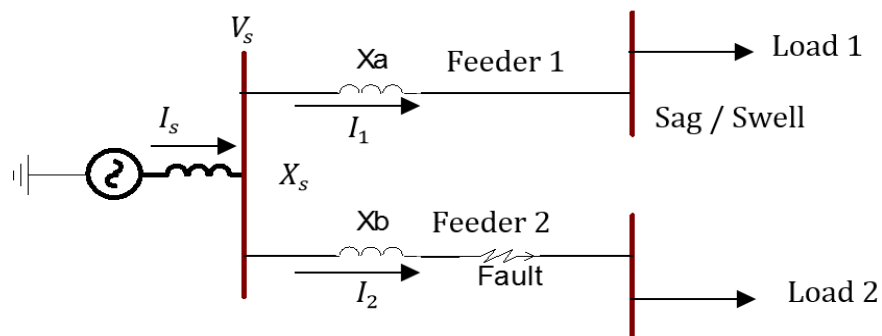

Fig. 2.15: Voltage sag / swell calculation schematics [26]

Under normal operation condition, the supply current, I_s;

$I_s = I_1 + I_2$ (Kirchhoff's Current Law, KCL)

$$I_s = \frac{V_s}{X_a + Z_1} + \frac{V_s}{X_b + Z_2} \tag{2.13}$$

$$V_1 = I_1 (X_a + Z_1) \tag{2.14}$$

$$V_2 = I_2 (X_b + Z_2) \tag{2.15}$$

When an open-circuit fault occurs on feeder 2 or a sensitive inductive load is suddenly connected, high current (open circuit current, I_o) tends to flow through feeder 1, thereby increasing its voltage. Equation (2.14) will become;

$$V_1 = (I_1 + I_o)(X_a + Z_1) \tag{2.16}$$

The voltage rise, $I_o(X_a + Z_1)$ is referred as voltage swell or momentary over-voltage [9].

In the case of short-circuit fault or connecting heavy capacitive load to feeder 2, more current is drawn by that feeder, thereby reducing feeder 1's current by short circuit current, I_s hence decrease in voltage. Equation (2.15) will now become;

$$V_1 = (I_1 - I_s)(X_a + Z_1) \tag{2.17}$$

This decrease in voltage, $I_s(X_a + Z_1)$ is referred as voltage sag or dip [26].

2.3.4.2 Series Voltage Injection

DVR operates by injecting converted AC voltage (V_{DVR}) in series (in phase or 180^0 out of phase) with the grid voltage V_s, thereby maintaining the load voltage at the desired reference level. Referring to Fig. 2.15, with Thevenin's equivalent circuit of the system.

$$Z_{th} = R_{th} + jX_{th} \tag{2.18}$$

$$V_S + V_{DVR} = V_L + Z_{th}I_L \tag{2.19}$$

It generates reactive power needed while the energy storage supply the active power.

$$I_L = \frac{P_L + jQ_L}{V_L} ;$$

$$S_{DVR} = V_{DVR}I_L^* \quad \text{(Complex power injected)} \tag{2.20}$$

Sinusoidal PWM-Based Voltage Source Converter

In both D-STATCOM and DVR control scheme, Sinusoidal Pulse Width Modulation (SPWM) based Voltage Source Converter (VSC) is used. There are many types of VSC depending on the number of levels or pulses; 6-pulse, 12-pulse, 24-pulse, 48-pulse, quisi-pulse and higher number of levels. As its basic application, VSC converts DC voltage to AC form just like an inverter.

Three phase, six pulse, two-level VSC (which is used in this thesis) consist of six power electronic valves; comprising of switching devices and anti-parallel diode with some snubber circuits. There are three arms that initiate the generation of three phase voltage of the VSC as shown in Fig 2.16, with each arm having two switching devices that are designed not to turn ON or OFF simultaneously.
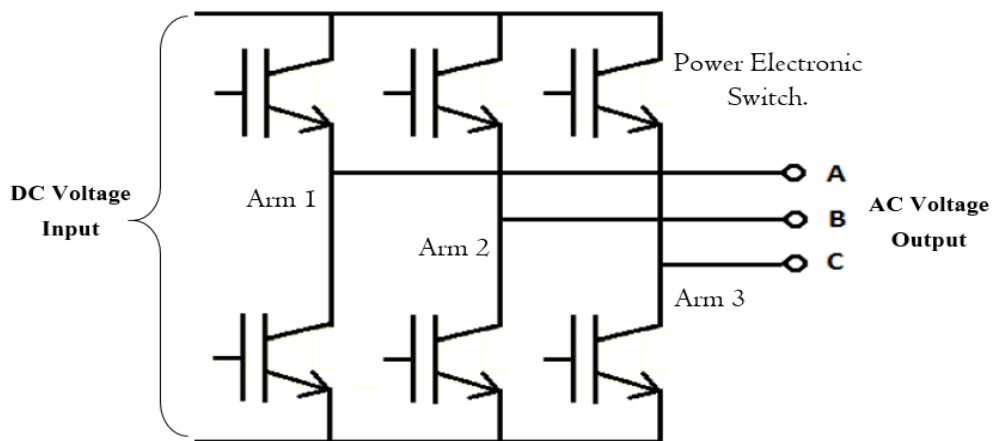
Fig. 2.16: Three phase 6-pulse voltage source converter [26]

Even though, many types of modulation exist like Pulse Amplitude Modulation, Pulse Position Modulation, Inverted Sine Pulse Width Modulation (ISPWM) and Space Vector PWM [9], in literature, however, SPMW proved to be the most efficient as it give the devices ability of independent control of real and reactive power, less power loss and fast response [17]. SPWM involves the superimposing a sinusoidal modulating signal (reference) on to a high frequency triangular (carrier) signal as depicted in Fig. 2.17. The instantaneous intersections between these two signals determine the switching pattern of the width-modulated pulses, V_o [14].

Fig. 2.17: SPWM with modulation index of 0.8 [14]

The ratio of these signals' amplitude and frequency called *amplitude modulation index,* m_a and *frequency modulation ratio,* m_f defined in Equations (2.21) and (2.22) respectively, play an important role in the operation of the VSC [18].
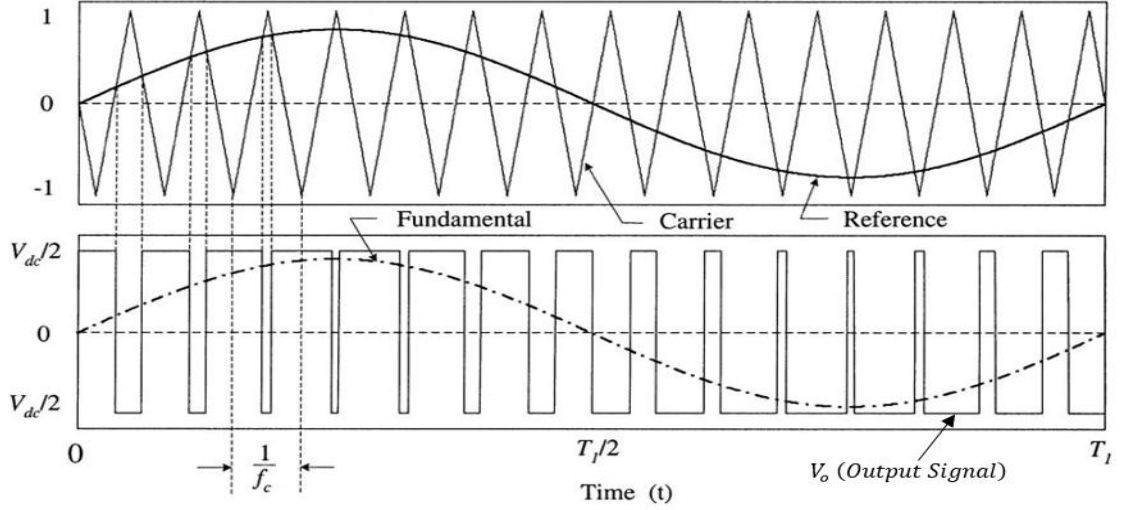
$$m_a = \frac{A_{sin}}{A_{tri}} \qquad\qquad\qquad (2.21)$$

$$m_f = \frac{f_{tri}}{f_{sin}} = 3k \ (k \in 2N + 1) \qquad\qquad\qquad (2.22)$$

A_{sin} , A_{tri}, f_{sin} and f_{tri} are amplitudes and frequencies of the modulating and carrier signal respectively. Table 2.6 summarizes the implication of this modulation indices.

Table 2.6: Implication of modulation indices on SPWM based VSC [14, 18]

Indices	Modulation	Consequences
$0 \le m_a \le 1$	Linear Modulation.	The output, V_o is a linear function of m_a and the VSC dc input, hence is the desired region of operation.
$m_a > 1$	Over Modulation.	The output no longer possess that linearity, and causes the carrier signal to undergo phase reversal.
$m_f = 3k$ $(k \in 2N + 1)$	---	It is advisable or rather necessary to choose large carrier frequency (mostly in the range of 2-15 kHz) and odd triple multiple of the modulating frequency. This significantly minimalize the harmonics content and prevent high frequency components to prevail.

CHAPTER THREE

SYSTEM DESIGN AND MODELLING

Among the requirements in power system point of view to achieve Smart Grid, two important features are demonstrated in the test system. These are:

➢ Power quality control.

➢ Integration of distributed generation to the electrical utility grid.

The model presented in this thesis to demonstrate the aforementioned applications of FACTS devices comprises of three important distinct models, together with their respective controls:

➢ FACTS Controllers; Distribution Static Synchronous Compensator (D-STATCOM) and Dynamic Voltage Restorer or Static Series Synchronous Compensator (DVR/SSSC).

➢ Distributed Generation; Photovoltaic Solar System (PSS) is selected due to its ubiquity.

IEEE1547 standard of regulating sensitive load voltage within $\pm$5% of the nominal value is abided in all the modeling and simulation discussed in this thesis. PSCAD/EMTDC software is used for the modelling and simulation of the system.

3.1 PSCAD/EMTDC SOFTWARE

Power System Computer Aided Design / Electromagnetic Transient including Direct Current (PSCAD/EMTDC) is a time domain software used for examining the behavior of electrical power systems, first developed in 1976 by Manitoba HVDC Research Centre. There similar simulation tools to PSCAD, like RSCAD and Simulink SimPowerSystems. RSCAD is the fastest compared to Simulink SimPowerSystems which gets slower with higher number of system components in a circuit design.

However, RSCAD is very expensive and memory consuming [22]. To compromise between the speed and the cost, PSCAD proved to be the best option, especially if its interfacing capability with MATLAB/SIMULINK is considered in addition.

PSCAD/EMTDC provides a graphical user interface, just like MATLAB/SIMULINK, with full library of typical and advanced components, numerous control tools and modules for some specific devices, allows the user to analyze, design and model systems in various configurations. Among the important components in PSCAD are:

- **Sources: -** Three and single phase AC and DC sources with internal and external control ability, Multiple Harmonic Current source and PV source with its controls.
- **Passive Elements:** - Fixed and variable resistors, inductors and capacitors. Single line to three phase splitter, ground, resistive, capacitive and inductive loads etc.
- **Breakers and Faults:** - Single and three phase circuit breakers. Balanced and unbalanced three phase fault with its Time Fault Logic.
- **Power Electronics/ FACTS/ HVDC**: - Diode, GTO, IGBT, Thyristor, Transistor, Static Var Compensator (SVC), Interpolated Firing Pulses Generator, 6-pulse HVDC System, 6-pulse Bridge, TSC/ TRC among others.
- **Power Transformers: -** Single and 3-phase transformers with variable windings.
- **Machines: -** Induction and Synchronous Machines, Steam and Hydro Governors, Power System Stabilizers, Turbine Control, DC machine, Permanent Magnet Machine, Wind Energy Source, DC, AC and static exciter models.
- **Logic Circuits: -** Multi-input Logic Gates, flip-flops, shift register and multiplexer.
- **Meters: -** Ammeters, Voltmeters, Multi-meter, Real and Reactive Power Meter, single and three phase RMS meters and On-line Frequency Scanner.

Simulations can be carried out in frequency domain if it's interfaced with SIMULINK.

3.2 D-STATCOM DESIGN REQUIREMENTS

As discussed in the previous chapter, D-STATCOM has three main components, namely;

- Energy Storage System (ESS)
- Voltage Source Converter and its controller
- Coupling Transformer

Design procedures and some reasonable assumptions that gives good results, are used to model some components in order to come up with the complete model of the D-STATCOM. Default values of some components in the PSCAD library are used also.

3.2.1 Energy Storage System

The ESS comprises of a capacitor which aid the power exchange between the AC system and the D-STATCOM. Some design assumptions are made prior to choosing the capacitor type. Its voltage, V_{dc} depends on the PCC voltage, V_s as shown in Equation (3.1) and must be greater than the AC bus voltage for proper operation of the VSC [18].

$$V_{dc} = \frac{3\sqrt{3}}{\pi} V_s \qquad (3.1)$$

V_{dc}: DC voltage across the capacitor.

V_s: Distribution bus AC voltage (at PCC).

For an 11.0 kV distribution system, with unity modulation index, the DC voltage is;

$$V_{dc} = \frac{3\sqrt{3}}{\pi} \times 11 = 18.19 \ kV$$

The value of the capacitor C_{dc} used is obtained using the relation shown in below [36].

$$C_{dc} = 3 \ \frac{V_s \Delta I_L T}{(V_{dcmax}^2 - V_{dc}^2)} \qquad (3.2)$$

V_{dcmax} = Pre-set upper limit of the DC link capacitor: is the maximum voltage across the capacitor, resulting from the power exchanges taking place between the D-STATCOM and the AC system sequel to load variation. Its difference with capacitor voltage, V_{dc} is chosen not to exceed 17% of the DC capacitor voltage.

ΔI_L = Step down of load current: is the difference between the load current before and during fault or sensitive loads. It is chosen not to exceed $\pm$ 10% of the load current.

At the D-STATCOM side, with coupling transformer of turns ratio 33/6.5kV.

$$\Delta I_L = \frac{33}{6.5} \times 1.98 = 10.05 \ A$$

T: is the period of the supply, given by;

$$T = \frac{1}{f}$$. (3.3)

For a 60Hz distribution system, *T= 16.667ms.*

V_s = 11.0kV, V_{dc} = 18.19kV, V_{dcmax} = 32.15kV and ΔI_L = 10.05A

$$C_{dc} = 3 \, \frac{11 \times 10.05 \times 1.667 \times 10^{-3}}{(32.12^2 - 18.19^2)} = 7.89 \times 10^{-4} F$$

Hence $800\mu F$ capacitor is chosen for the DC link energy storage as depicted in Fig. 3.1.

Fig. 3.1: PSCAD model of DC link capacitor with a multi-meter

3.2.2 Voltage Source Converter

6-pulse VSC is used for the purpose of this thesis, even though higher number of pulses like 12, 18, 24, 48, 84 and 92 pulses exist, but present a lot of design complexities. 6-pulse VSC uses 2 switching devices per phase, as shown in Fig. 3.2.
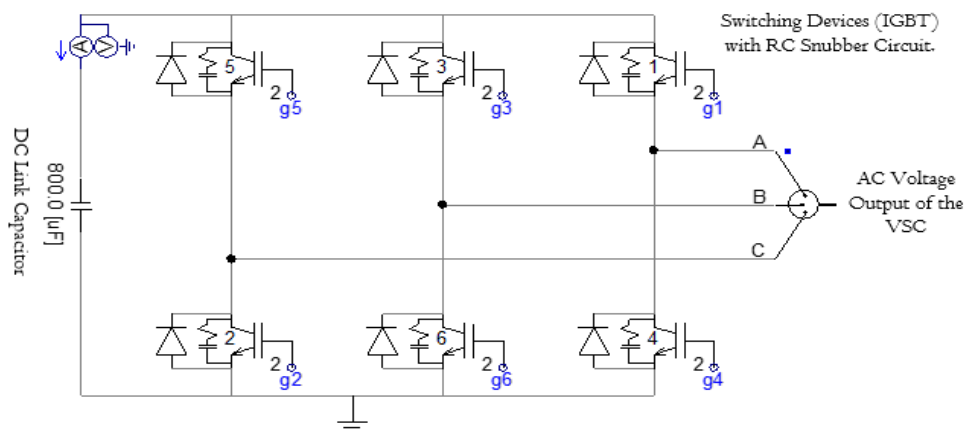

Fig. 3.2: PSCAD model of six-pulse voltage source converter

There are many types of power switching devices; Gate Turn-off Thyristor (GTO), Insulated-gate Bipolar Junction Transistor (IGBT), Metal Oxide Semi-conductor Field-Effect Transistor (MOSFET), and MOS Controlled Thyristor (MCT) among others, but

IGBT proved to have higher current handling capacity, voltage ratings and smaller ON-state voltage drop than the rest of the devices [18]. Hence IGBT, coupled with RC-snubber circuit as shown in Fig 3.3, are chosen. The RC snubber are introduced to minimize switching losses by altering the switching trajectory, while the shunt diode is used to lock the unfiltered output pulses of the VSC after switching and provide path for inductive current whenever the IGBTs in the same arm are turn off [4].
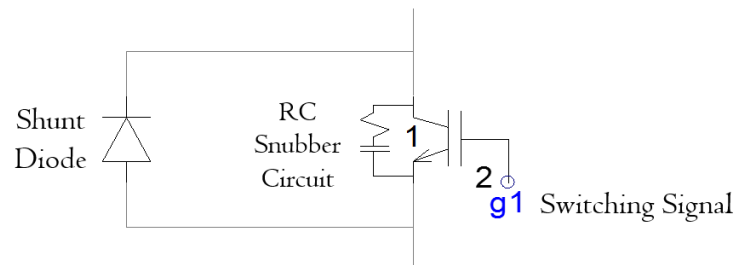

Fig. 3.3: IGBT, shunt diode and RC snubber circuit

Default values of the IGBT data and that of the snubber circuit model in PSCAD, shown in Fig 3.4, are used for the design and simulation.
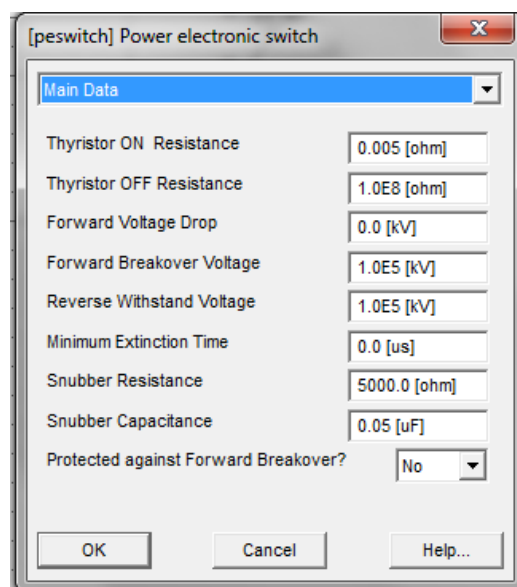

Fig. 3.4: IGBT and RC snubber circuit data (default) in PSCAD

3.2.3 Sinusoidal Pulse Width Modulation (SPWM)

To generate the suitable firing pulses that governs the operation of the VSC, Sinusoidal Pulse Width Modulation (SPWM) is selected. This is due its little power consumption while in operation and mainly used for high power application which make it versatile and common in modern converter design [14, 18]. SPWM presented in this thesis sub-categorize in to:

➢ Voltage control
➢ Modulation signal generation
➢ Carrier signal generation
➢ Firing pulses generation

3.2.3.1 Voltage Control

To preserve a constant voltage magnitude at the PCC, the voltage control system shown in Fig. 3.5, measures the r.m.s voltage, V_{rms} p.u at the PCC and compare it with a reference voltage signal (1.0 pu is chosen) thereby establishing an error signal. Proportional-Integral (PI) controller process this error signal and generates a required phase shift, δ which will lessen the error.
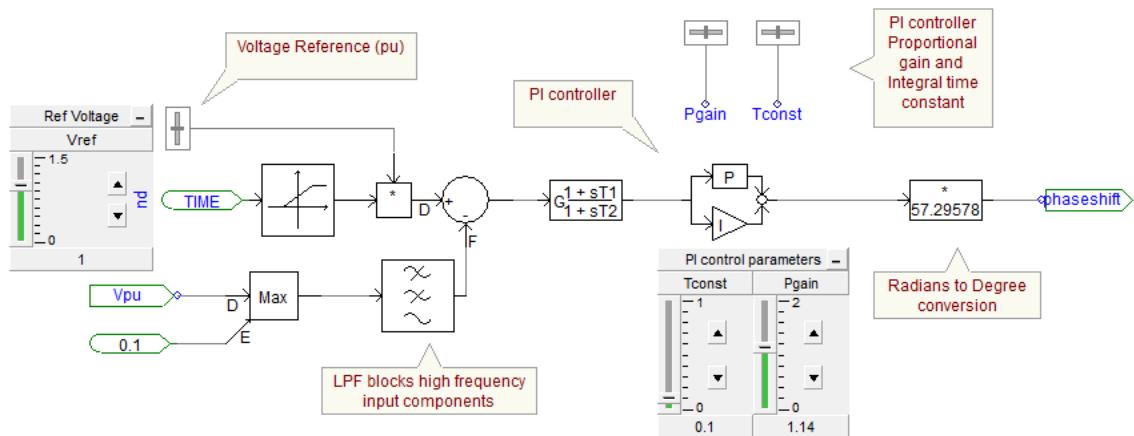

Fig. 3.5: Voltage control circuitry

The PI controller proportional gain and integral time constant are adjusted to optimum value in order to obtain accurate switching pulses.

3.2.3.2 Modulation Signal Generation

Fig. 3.6 shows the circuit used to generates the sinusoidal signal. Linear ramp outputs are obtained from the six pulse Phase Locked Loop (PLL) that varies from 0^0 to 2π rad. These outputs are then shifted by the PI output angle, δ and $\pi/6$ shift.
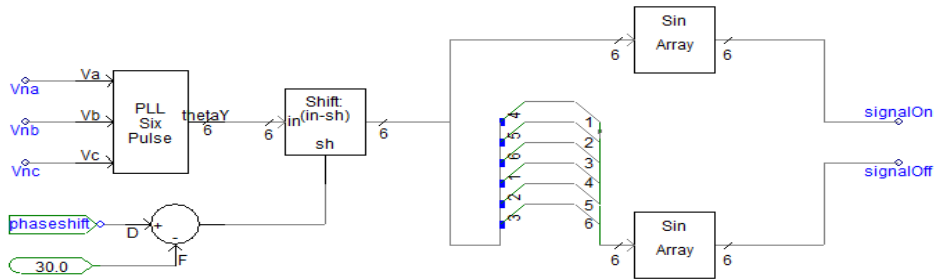

Fig. 3.6: Sinusoidal waveform generator

Unity amplitude modulation index, m_a is chosen to ensure linear modulation. The gains of the PLL are also adjusted to obtain their optimal values shown in Fig 3.7.
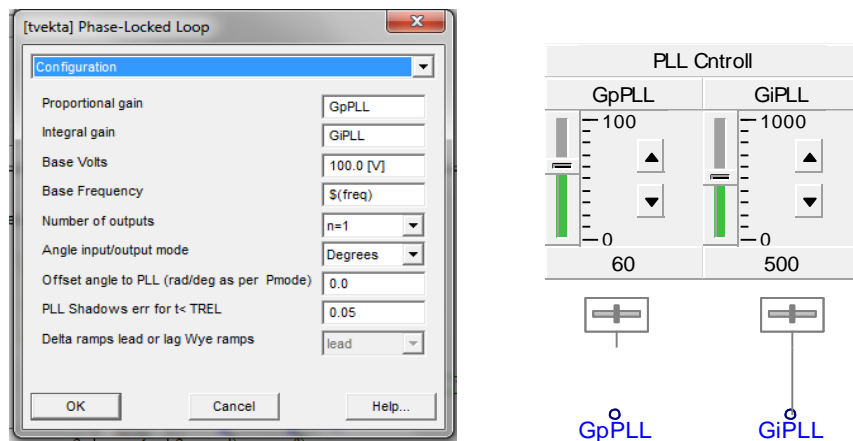

Fig. 3.7: PLL proportional and integral gain values in PSCAD

3.2.3.3 Carrier Signal Generation

High frequency carrier signal (Triangular wave) is obtained from the circuit shown in Fig. 3.8. The *frequency modulation ratio* of 39 is chosen ($m_f = 39$). With modulating signal frequency, $f_{sin} = 60Hz$, the carrier signal frequency is $f_{tri} = 60 \times 39 = 2.34\ kHz$. It is taken high enough to reduce the level of harmonics.
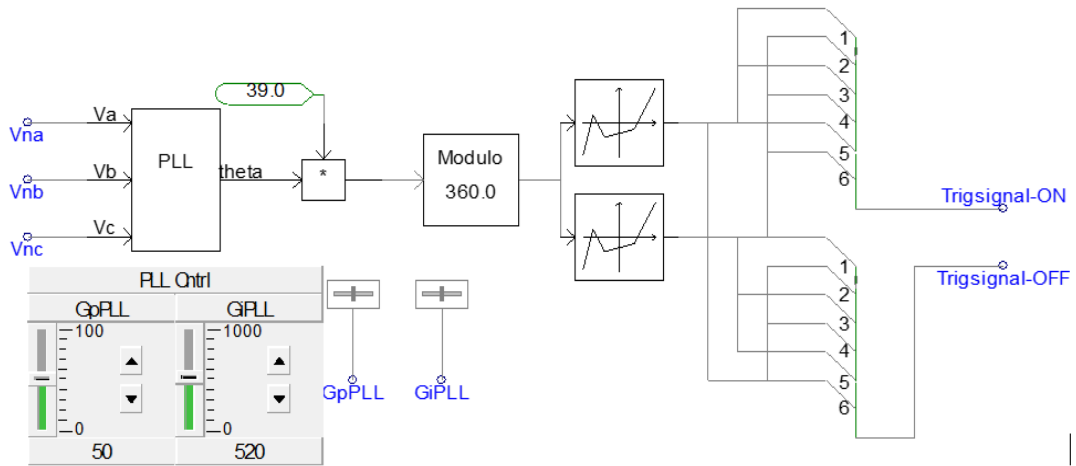
32

Fig. 3.8: Triangular wave generation

3.2.3.4 Firing pulses generation

Finally, the sinusoidal signal (signal-ON and signal-OFF) and the carrier signal (Trisignal-ON and Trisignal-OFF) obtained from the circuits depicted in Fig. 3.7 and Fig. 3.8 respectively, are feed in to Interpolated Firing Pulse Generator shown in Fig. 3.9, to obtain the required firing pulses (g1, g2 ..., g6).
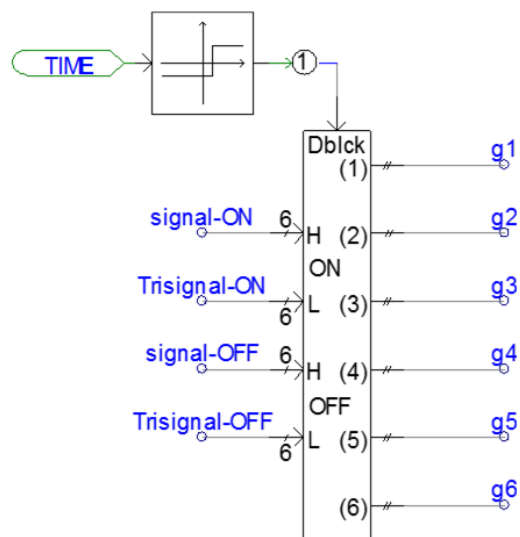

Fig. 3.9: Interpolated firing pulse generator

These firing pulses with different switching pattern triggers the IGBTs used in the volatage source converter, via the gates. It is designed in such away that two IGBTs on the same leg (like IGBT2 and IGBT5) do not turn ON or OFF simulteneously.

3.2.4 Coupling Transformer

Careful considerations are taken to achieve suitable real and reactive power exchanges between the DSTATCOM and the AC system via the reactance of the coupling transformer. A 3-phase, 33/6.5, 5MVA, $Y - \Delta$ connected transformer shown in Fig. 3.10 is chosen for the purpose of coupling the device to the network (in shunt) and transforming its voltage level at PCC to align with that of the network.
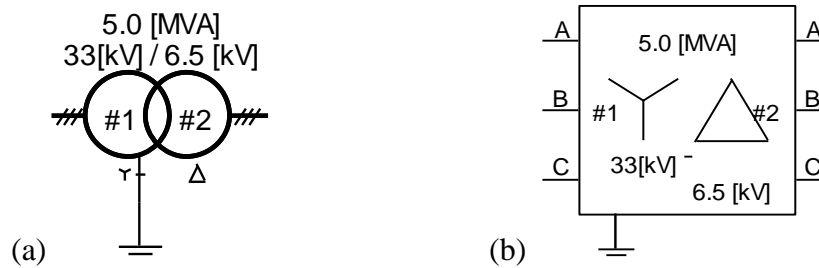

Fig. 3.10: PSCAD model of coupling tranformer (a) Single line (b) Three phase view

It is modelled with a leakage reactance of 15% to minimize the flux leakage in the model. $Y - \Delta$ connection is to maximize the output voltage of the DSTATCOM. The parametric data of the transformer is shown in Fig. 3.11 below.
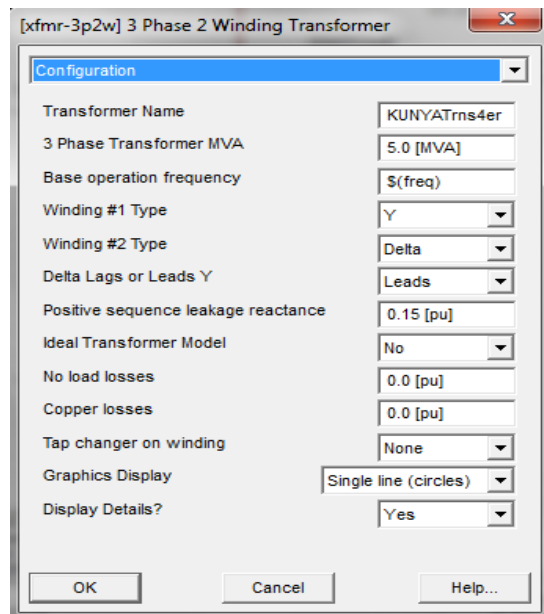

Fig. 3.11: Coupling transformer parameters on PSCAD

Having the DC link, VSC with its SPWM control and the coupling transformer well modeled, the complete model of the DSTATCOM is shown in Fig. 3.12.
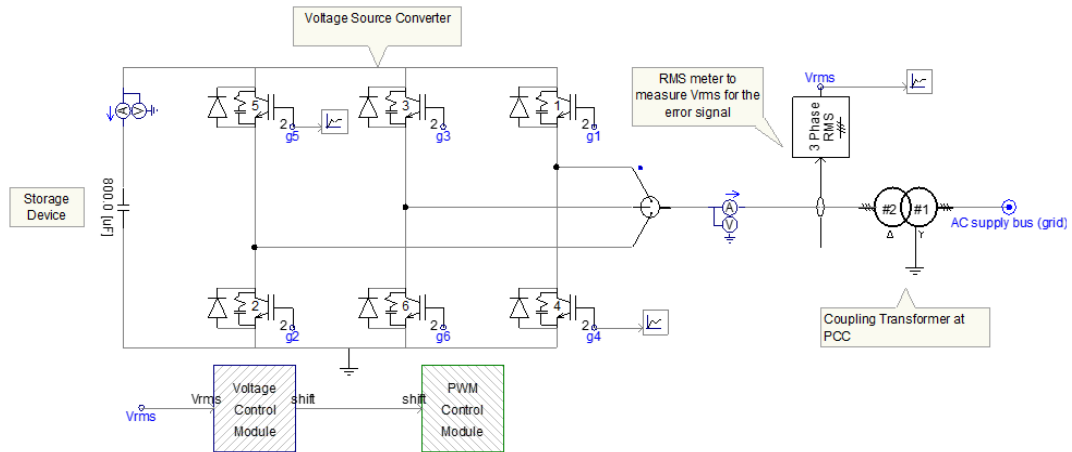

Fig. 3.12: Complete PSCAD model of 6-pulse D-STATCOM

3.3 DVR DESIGN REQUIREMENTS

As discussed in the previous chapter, DVR has similar configuration with D-STATCOM, with the latter being connected in shunt mode with the main AC network and the former in series via the reactance of coupling transformers. Similarly, DVR has some basic components which build up the complete DVR model. These components are:

➢ Energy Storage System
➢ Voltage Source Converter and its controller
➢ Voltage Injection Transformer
➢ By-pass Switches

Design decisions are discussed prior to coming up with complete model of the device.

3.3.1 Energy Storage System

Among the important features to consider while modelling ESS is not only prompt response ability of the system to sudden load variation but also prolonged voltage support when the disturbance persist. In that case, ESS of DVR often consists of a battery that gives active power support to the VSC.

35

In most cases, DVR is operated at medium voltage level, hence 15kV DC input voltage is chosen for the purpose of modelling. This falls within the typical and commonly DVR-installed systems voltage ratings of 11kV to 63kV [16]. Since DVR is one of the custom power devices, the energy storage within the range of 0.11MJ to 11MJ should be chosen, as describe in Table 2.5 in the previous chapter. Hence 0.22MJ is chosen as the energy stored. With the DC link voltage, V_{dcdvr} chosen to be 15kV, the DC link capacitance can be evaluated using Equation 3.4.

$$C = \frac{2E}{V_{dc}^2} \qquad\qquad\qquad .(3.4)$$

$$= \frac{2 \times 0.22 \times 10^6}{15000^2} \quad = \quad 22.45mF$$

Hence $2250\mu F$ capacitor is chosen as DC link capacitor and ideal DC voltage source modelled the battery as shown in Fig. 3.13.
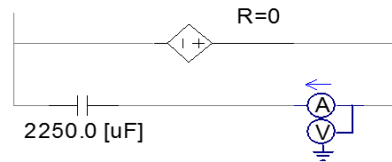

Fig. 3.13: DVR energy storage on PSCAD

3.3.2 Sinusoidal Pulse Width Modulation of DVR's VSC

Unlike in D-STATCOM's VSC where some circuits are modelled to generate the individual signals; modulating and carrier signal, the VSC modelled in DVR employs the use of discrete component in the PSCAD library to generate the carrier signal and the sinusoidal modulating signal. These signals are then super-imposed with one another to generate the required switching pulses for the IGBTs.

3.3.2.1 Carrier Signal Generation

As in the previous case, triangular carrier signal with high frequency, which lies in the desired range of 2-15 kHz for switching power systems, is used for the purpose of this modulation. Fig. 3.14 (a) shows the PSCAD model of the triangular signal generator.
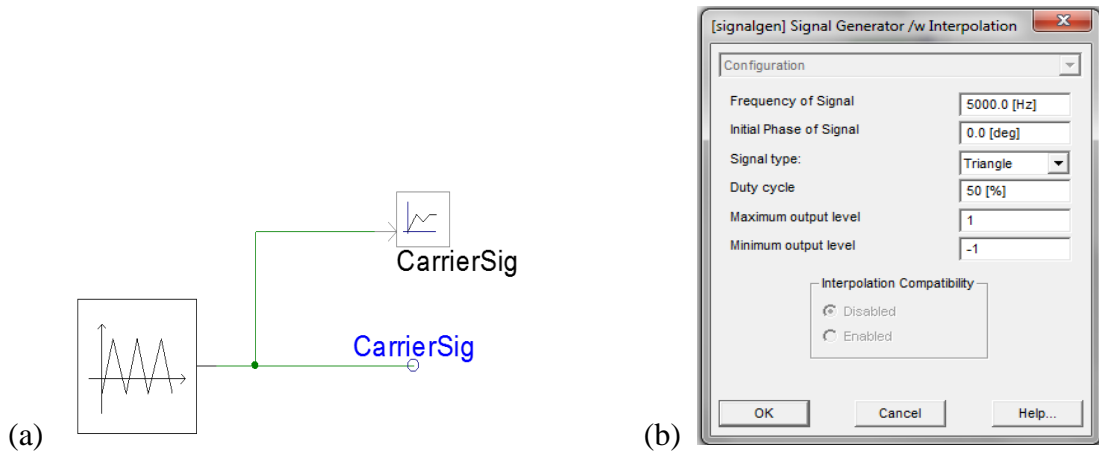
Fig. 3.14: PSCAD model of triangular signal generator and its configuration data

High frequency of 6kH is chosen to minimize the level of harmonics from intruding the VSC. Default value of the generator duty cycle of 50% as it is in the PSCAD library is used, and luckily give a remarkable results. The signal's maximum and minimum default levels are 1 and -1 respectively as shown in Fig. 3.14 (b).

3.3.2.2 Modulating Signal Generation

Three sinusoidal wave generators are used to generate the 3-phase modulating signals as shown in Fig. 3.15. This approach gives room for specifying the magnitude, phase angle and frequency of each phase. This is useful in correcting unbalance faults.
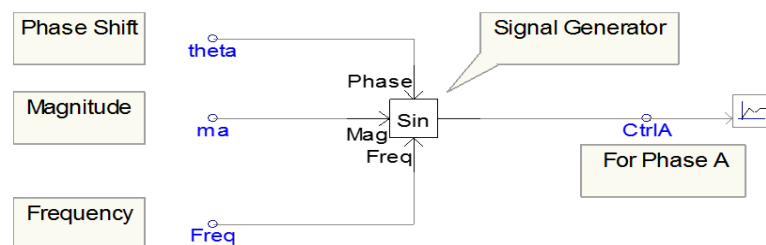

Fig. 3.15: Sinusoidal modulating signal generation for single Phase (A)

The main advantage of this modulation is that, the magnitude of these sinusoids can be varied to have an unbalanced VSC output if desired. In this thesis, balanced output is chosen, hence equal magnitude and frequency are given to all the three sinusoidal waves

as shown in the phasor representation of Fig. 3.16 below. The phases are then spaced by angle of $2\pi/3$ rad (120^0), as depicted in Equation 3.5.
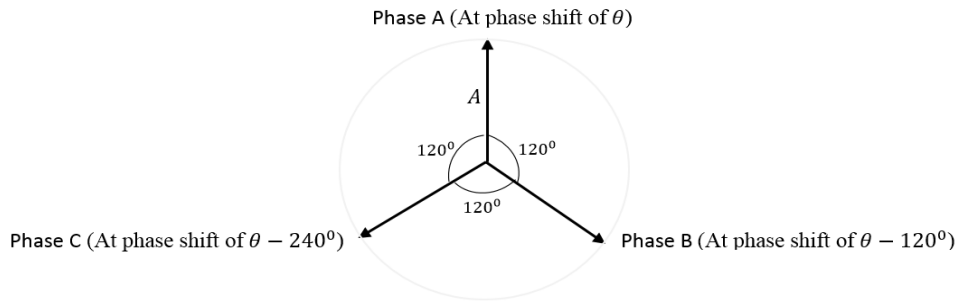

Fig. 3.16: Phasor representation of three phase voltages spaced by 120^0 degrees

$$V_a = A\sin(\omega t + \theta)$$

$$V_b = A\sin(\omega t + \theta - 2\pi/3) \hspace{3cm} (3.5)$$

$$V_c = A\sin(\omega t + \theta + 2\pi/3)$$

Where A, θ and ω are the magnitude, phase angle and frequency of three sinusoidal modulating signals. With the magnitude, A = 1, the circuitry below modeled Equation 3.5, which provides the required sinusoids for the three phases.
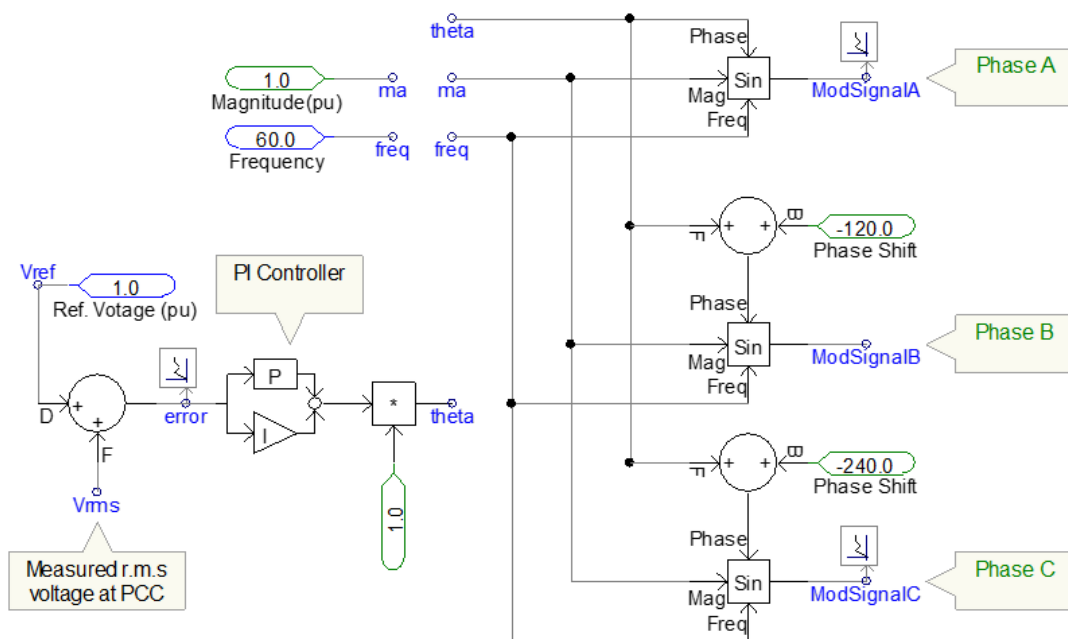

Fig. 3.17: Three phase modulating signal generation

The phase shift, theta is obtained by processing an error obtained by comparing the measured r.m.s voltage at the PCC with a reference signal. The reference signal is chosen to be 1.0 p.u, thus, the voltage at the PCC is to be maintained at 1.0 p.u approximately.

These signals are then fed into a comparator for the purpose of superimposing the modulating signal on the carrier signal as shown in Fig. 3.18. This will in turn generate pulses for each phase as shown in Fig. 3.19. As earlier mentioned, two IGBTs on the same leg (like IGBT2 and 5) do not turn ON or OFF simultaneously, hence gating pulse of a given IGBT is inverted to obtain the gating pulse of the other IGBT on the same leg.
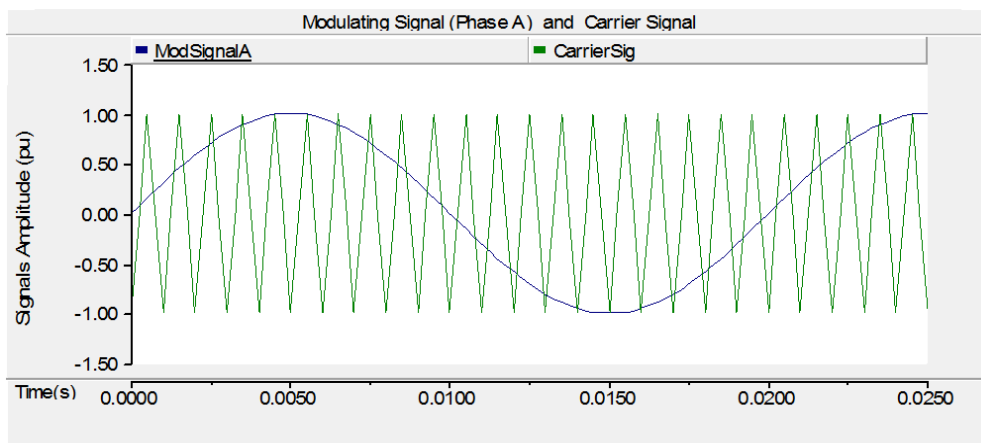

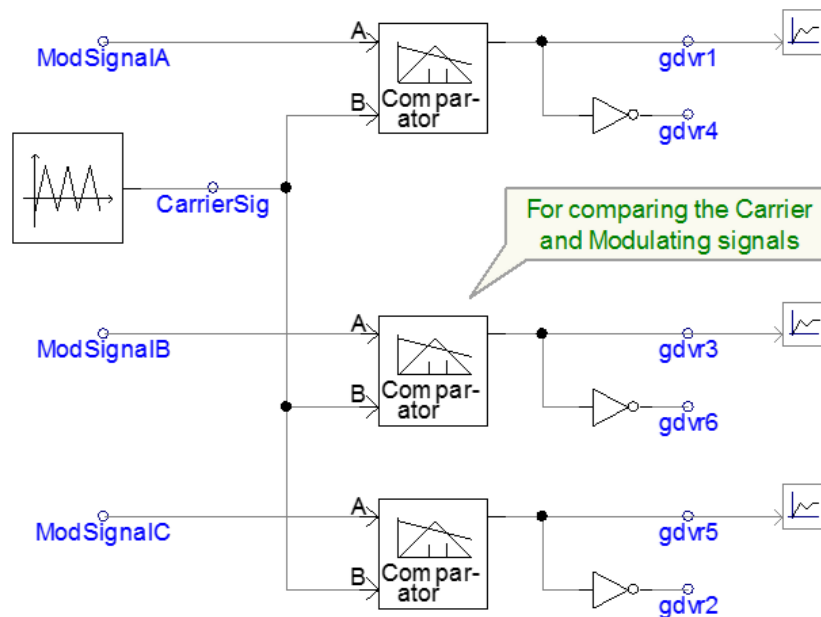Fig. 3.18: Phase-A modulating signal superimposed on the carrier signal

Fig. 3.19: DVR-VSC firing pulses generation

3.3.3 Series Injection Transformer

Three single-phase transformers are used to connect the DVR to the network, through which the three phase voltage produced by the VSC can be injected. They also provide the DVR an ability to operate in stand-by mode or boost / injection mode [29]. It is in stand-by mode when there is no any interruption in the network, hence DVR injects no voltage. In this mode, low-voltage winding is shorted through the converter. But when there any disturbance in the network, the DVR injects series voltage through the reactance of the transformer, hence operated in boost or injection mode. A three single-phase transformers shown in Fig. 3.20, each rated as 33/14, 7.5MVA, $Y - \Delta$ connected with the leakage reactance of 15% are used as the DVR's injection transformers.
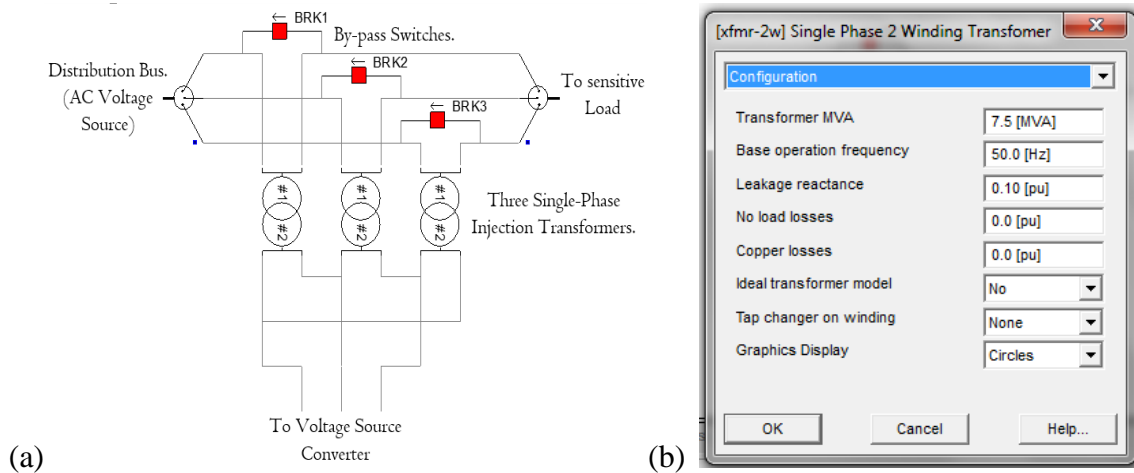

Fig. 3.20: PSCAD model of three single-phase DVR injection transformers

3.3.4 By-Pass Switches

Three single phase breakers, BRK1, 2 and 3 shown in Fig. 3.20 with very high OPEN resistance and very low CLOSED resistance of 1MΩ and 0.005Ω (default values in PSCAD library) respectively, are used for isolating the DVR if the current on the load side surpasses an acceptable limit due to a short circuit on the load or large inrush current [30]. Fig. 3.21 below shows the complete PSCAD model of 6-pulse, two-level DVR.
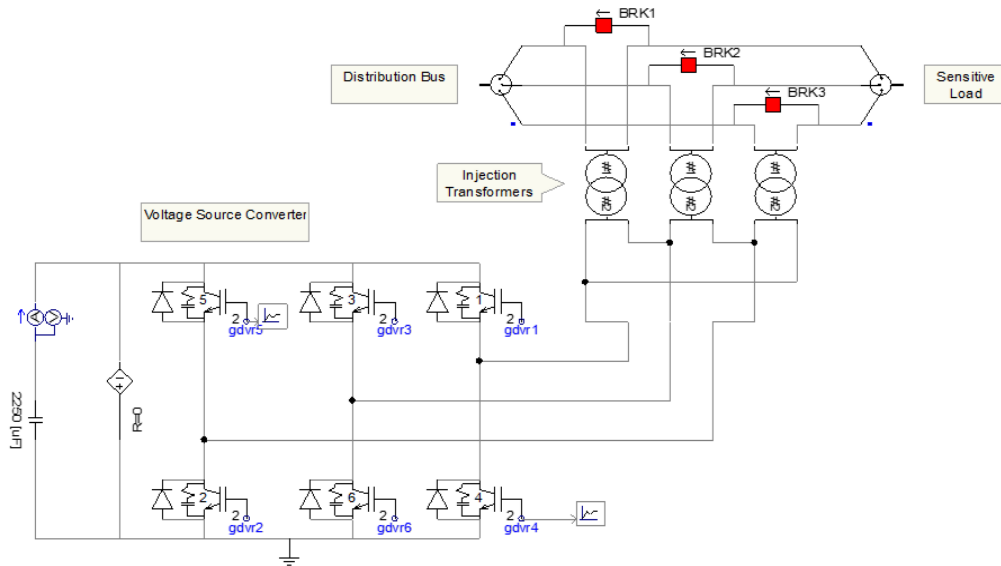
Fig. 3.21: Complete PSCAD model of 6-pulse DVR

3.4 PHOTOVOLTAIC SOLAR SYSTEM

To demonstrate the behavior of distributed generation source (one important feature of Smart Grid), a photovoltaic solar system is modeled. IEEE 1547.3 is abided while modeling the PSS. The scope of this thesis does not go in details about the PV system model concerning issues like Maximum Power Point Tracking (MPPT), Harmonic Distortion Analysis etc. Five major building components of PSS are modeled prior to finalizing the complete model. These includes;

- ➢ Solar Cell Array (As the source)
- ➢ DC link Capacitor
- ➢ Inverter and Filter
- ➢ Coupling Transformer

3.4.1 Solar Cell Array

PV module with some default parameters in the PSCAD library, developed by A. D. Rajapakse, is used as the solar cell array. While some parameters are altered to obtain better results. It is modeled to give a rated output voltage of 270V and the power of 1.0MW as in data sheet. The input parameters to this array are the temperature and the solar radiation as shown in Fig. 3.22.
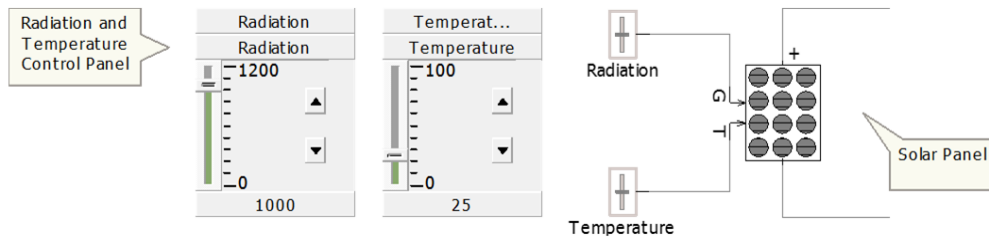
Fig. 3.22: Solar Panel with its Parametric Control Panel

The array is made up of a 45 parallel strings each of 50 modules serially connected as summarized in Fig. 3.23, making a total of 1550 modules each consisting of 108 cells as PSCAD defaults. These are chosen to obtain the desired output power and voltage level. The simulation is carried out at Standard Test Conditions (STC) in which the system is tested under the irradiance intensity of 1000 W/m^2, AM1.5 solar reference spectrum and cell temperature of 298K (25°C) [22]. Under this condition, each module is designed to generate 650W approximately, hence 1550 modules are needed to generate 1.0 MW.
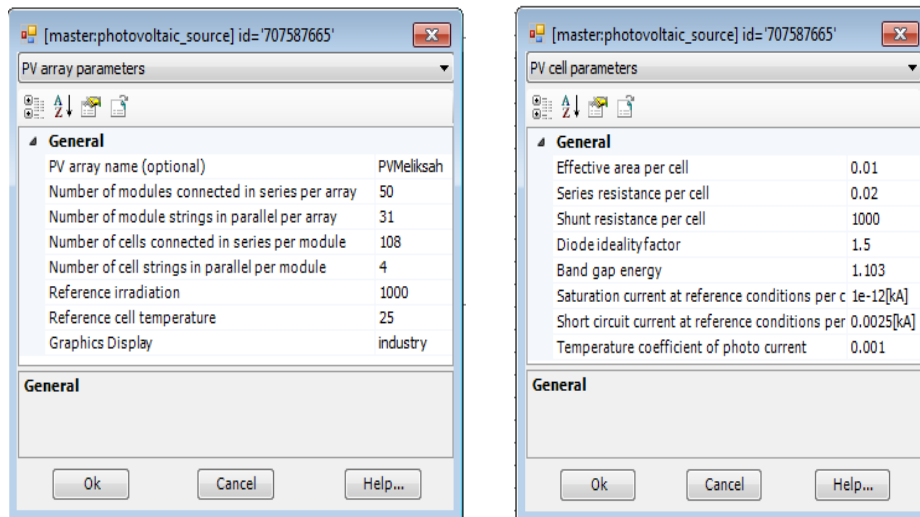
Fig. 3.23: Photovoltaic array and cell parameters on PSCAD

3.4.2 DC Link Capacitor

To minimize the ripples in the output voltage or rather power of the solar panel, a capacitor is placed between the solar panel and the inverter. It serves as sink and source every half cycle to help create a balance of power on the DC bus, hence it can be seen as an energy storage. It also generates reactive power in the absence of compensators.

In this thesis, 15.0 mF capacitor is used for such application. This capacitive value is not a calculated, but is obtained by trying several values with which the selected one present the best or at least a good result.

3.4.3 Inverter Design

3-phase, 2-level inverter shown in Fig. 3.24, is modeled to convert the generated DC power from the solar panel to AC. This is necessary in order to match the frequency and the voltage type to the utility grid (in the case of grid connected type). The output of the inverter is then connected to the grid via the filter and the coupling transformer.
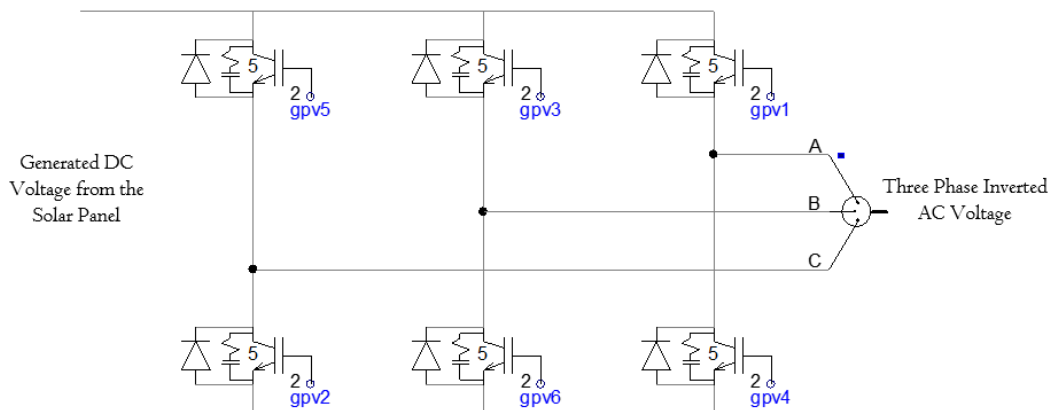

Fig 3.24: PSCAD model of three phase inverter for PSS

Default data values of the IGBTs, snubber circuits and the clamping diodes as consigned in the PSCAD library are used in this model. In order to provide the necessary gating signals of the switching devices, simple PWM is used. It begin by generating the modulating and triangular carrier signal shown in Fig. 3.25 below.
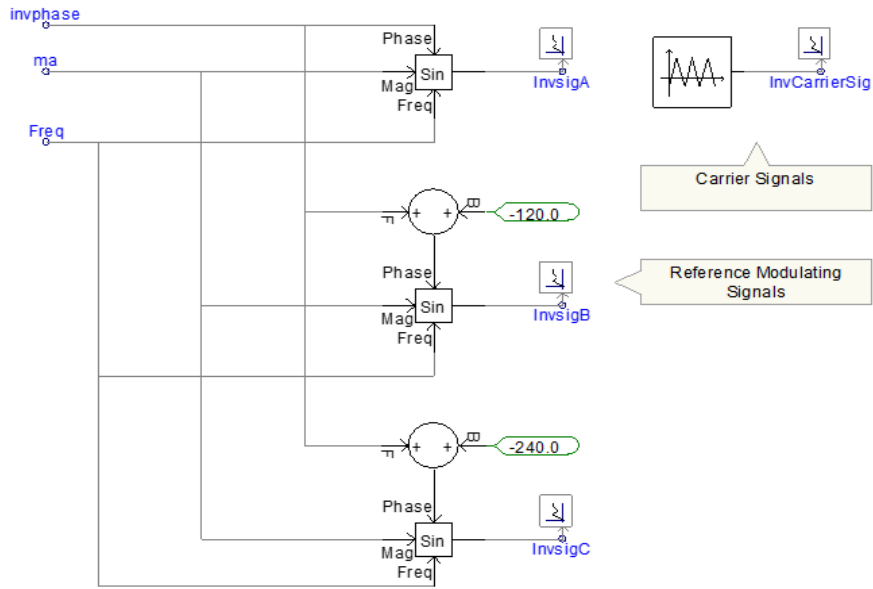
Fig. 3.25: Modulating and triangular carrier signal generation

The modulating signal and triangular carrier signals generated are then applied to the interpolated firing pulse generator in the pattern depicted in Fig. 3.26, to generate the gate switching signals.

Fig. 3.26: Firing pulses generation for PSS on PSCAD
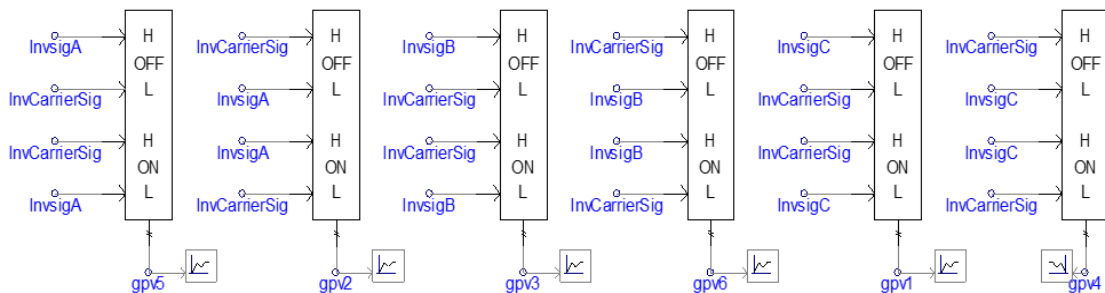
3.4.4 Filter Design

To improve the quality of the voltage and current generated by the PSS before injecting it to the grid, simple first order low pass L-C filter is designed for this purpose. It is also used extract the fundamental component and mitigate the higher frequency content as in [39]. $85\mu F$ inductor and $1.0mF$ capacitor are used as the filter components.
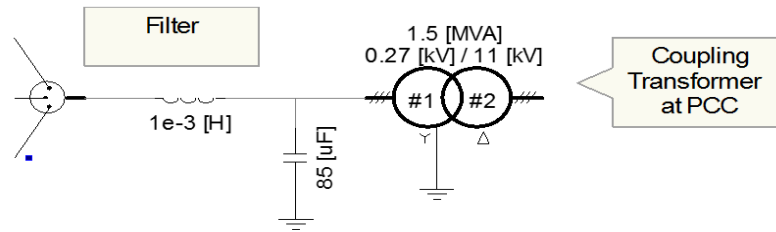
Fig. 3.27: Single line diagram of filter component and transformer on PSCAD

3.4.5 Coupling Transformer

To step up the voltage to the nominal value of the grid and provide a galvanic isolation between the PV system and the AC network, a three phase, two-winding, step-up transformer is used. The peak generation of the PSS determine the transformer ratings, taking the reactive power generated by the DC link capacitor and the inverter into consideration. Hence the power rating of the transformer should be more than that of the PSS generation to suppress such effects.

An ideal, 1.5 MW, 60Hz, $Y - \Delta$ transformer with a transformation ratio of 270V / 11kV is used. This is chosen by taking the inverters output voltage of 270kV and the utility grid voltage of 11kV to which the PSS is to be coupled. The $Y -$ connected primary winding is grounded and connected to the inverter, while $\Delta -$ connected secondary winding is linked to the grid, as shown in Fig. 3.27.

After modeling the individual units that build up the system, the complete model of the PSS is shown in Fig. 3.28. Simple model is used since the goal of this study can be accomplished without other complex modelling structures like MPPT and THD.
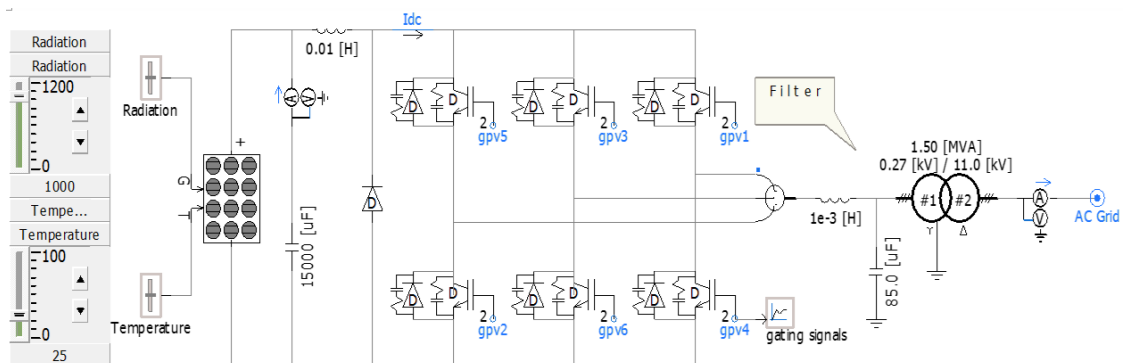

Fig. 3.28 Complete grid-tied PSS in PSCAD

45

CHAPTER FOUR

SIMULATIONS AND RESULTS

To demonstrate the capabilities and contributions of these two devices modeled; D-STATCOM and DVR towards achieving Smart Grid, two important tests are carried out on the individual devices. Two important features of Smart Grid are considered for these tests, thus:

- ➢ Power Quality Control through voltage stability
- ➢ Integration of Dispersed Generation Sources

4.1 TEST ON D-STATCOM

Three distinct tests are carried out on D-STATCOM to ascertain its effectiveness, namely:

- ➢ Voltage Sag Mitigation
- ➢ Voltage Swell Alleviation
- ➢ Grid-tied PSS power control

4.1.1 Voltage Sag Mitigation Using D-STATCOM

The test system comprises of 2-bus distribution system subjected to sensitive load variation and some three phase balanced faults. These sensitive loads (comprising of resistive and inductive loads) cause the system's voltage to change (decreases) thereby effecting its stability and that of the power quality. The D-STATCOM is later connected with a view of alleviating these problems through the exchange of real and reactive power between the device and the AC system at the point of common coupling, PCC. The circuit diagram illustrated in Fig. 4.1 shows the test system used to demonstrate the ability of D-STATCOM in alleviating voltage sags (dips).

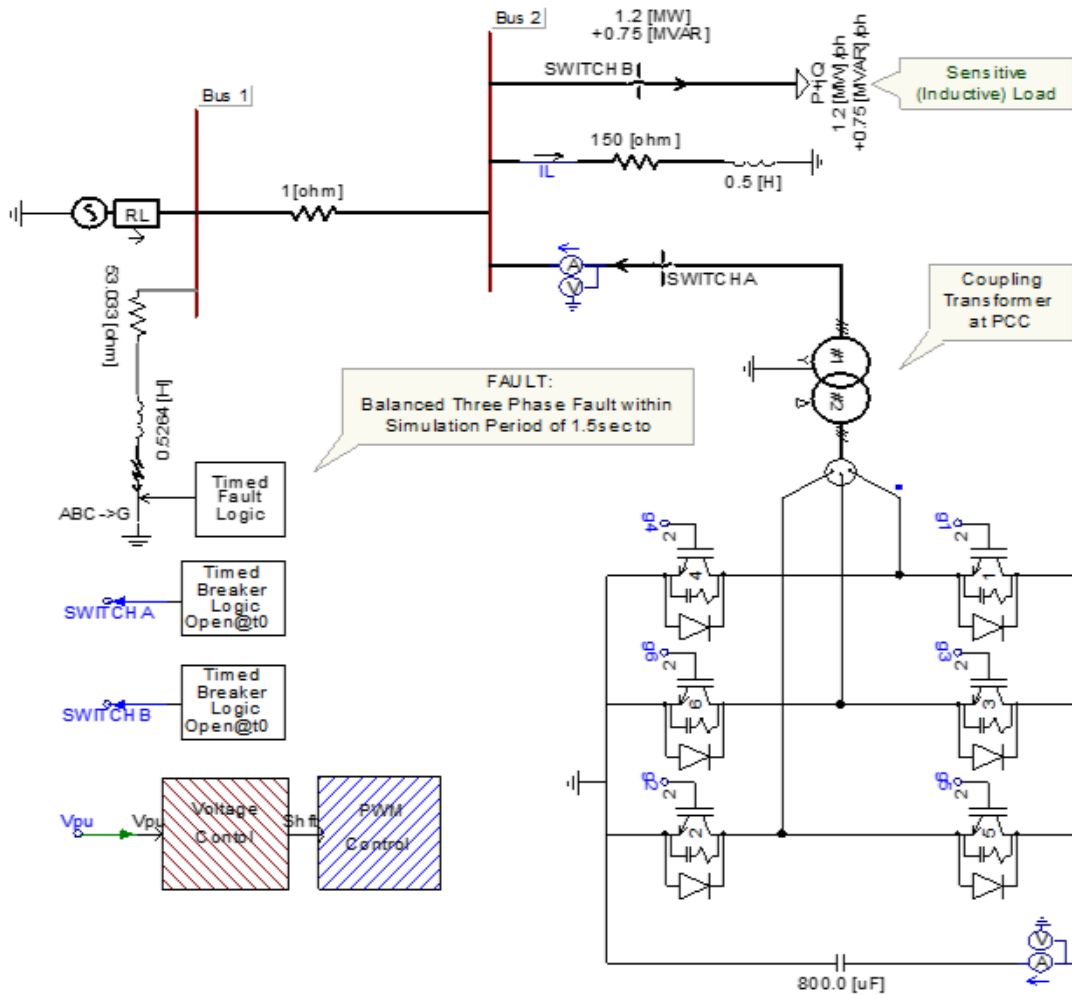Fig. 4.1: D-STATCOM voltage sag mitigation test system

The system's parameters are tabulated in Table 4.1.

Table 4.1: Test System Parameters

Parameter	Value
System Voltage.	$11.00\ kV$
Frequency.	$60Hz$
Sensitive Load	$(1.2MW + j0.75MVAR)/Phase$
Load Power Factor	0.85 Lagging
Fault Impedance	$(53.033 + j0.5264)\Omega$
Overall Simulation Time	2.50 Seconds

Two set of simulations are carried out; the first test is carried out without the D-STATCOM by opening switch A. In addition to that;

(a) An inductive load shown in Fig 4.1, is connected by closing Switch B within a simulation period, t_s of $0.5 \leq t_s \leq 1.00$sec. This causes the voltage to drop by almost 20% of the nominal voltage as shown in Fig. 4.2 below. This clearly shows a voltage sag or a dip. Line impedance has already dropped the voltage to virtually 8%.

(b) A balanced three-phase fault is introduced at 1.5sec which lasted for additional 0.50sec. It has similar effect as the sensitive inductive load described in (a) above, by decreasing the voltage level by roughly 19% of the reference voltage magnitude. This is to demonstrate two main sources of voltage sag, that is sudden connection of a sensitive load and fault which can likewise be an unbalance fault.
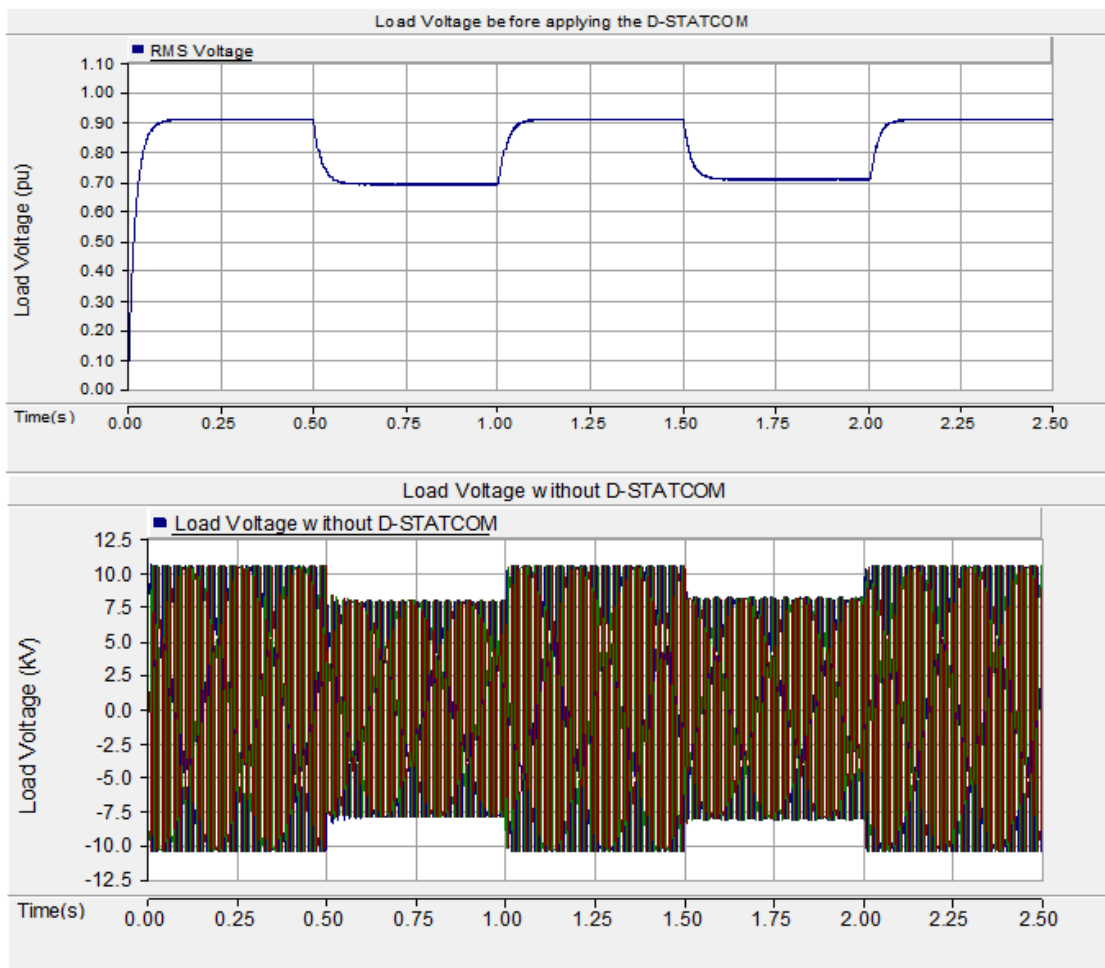

Fig. 4.2: Load voltage without the D-STATCOM

While the second simulation is carried out with the D-STATCOM by closing switch A to ascertain its effectiveness. The VSC generated three phase voltages during the voltage dip restoring the load voltage to its nominal voltage of 1.0 p.u level by clearing the sagging as shown in Fig. 4.3 and summarized in Table 4.2.
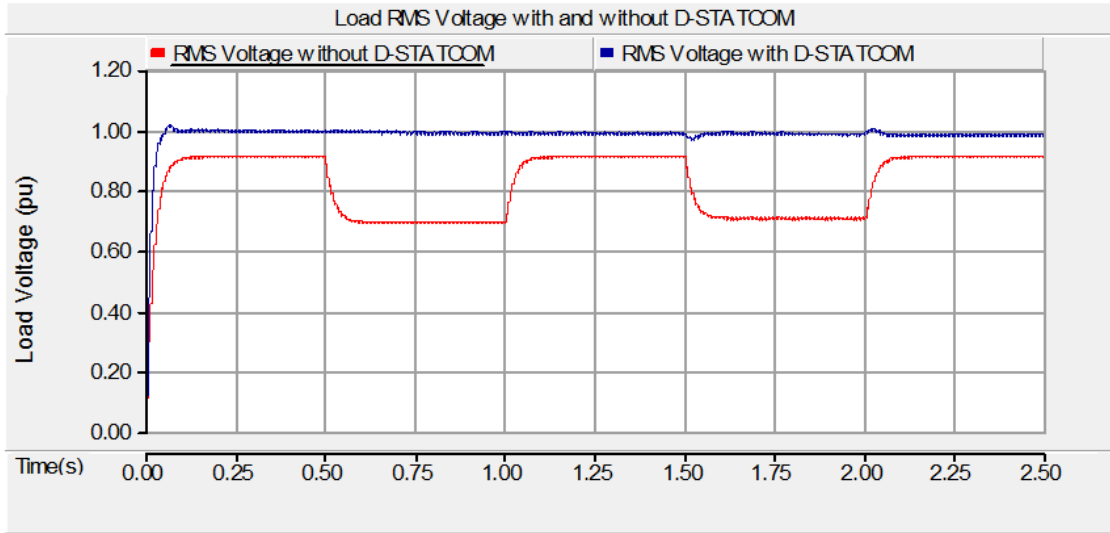

Fig. 4.3: RMS Load voltages with and without the D-STATCOM

Table 4.2: Summary of voltage dips mitigation using D-STATCOM

Parameter	Simulation Time (s)	Without D-STATCOM	With D-STATCOM
Load RMS Voltage (pu)	Without voltage dips	0.921	1.000
	$0.50 \leq t_s \leq 1.00$	0.709	0.981
	$1.50 \leq t_s \leq 2.00$	0.722	0.995
Load Instantaneous Voltage (kV)	Without voltage dips	10.131	11.00
	$0.50 \leq t_s \leq 1.00$	7.799	10.791
	$1.50 \leq t_s \leq 2.00$	7.942	10.945

These voltage corrections are within the ±5% range of IEEE 1549 Standard of voltage regulation. To clearly observe the load voltage waveform during the compensation, a close-up view of the instantaneous load voltage within a simulation period of $0.45 \leq t_s \leq 0.55$sec is illustrated in Fig. 4.4.
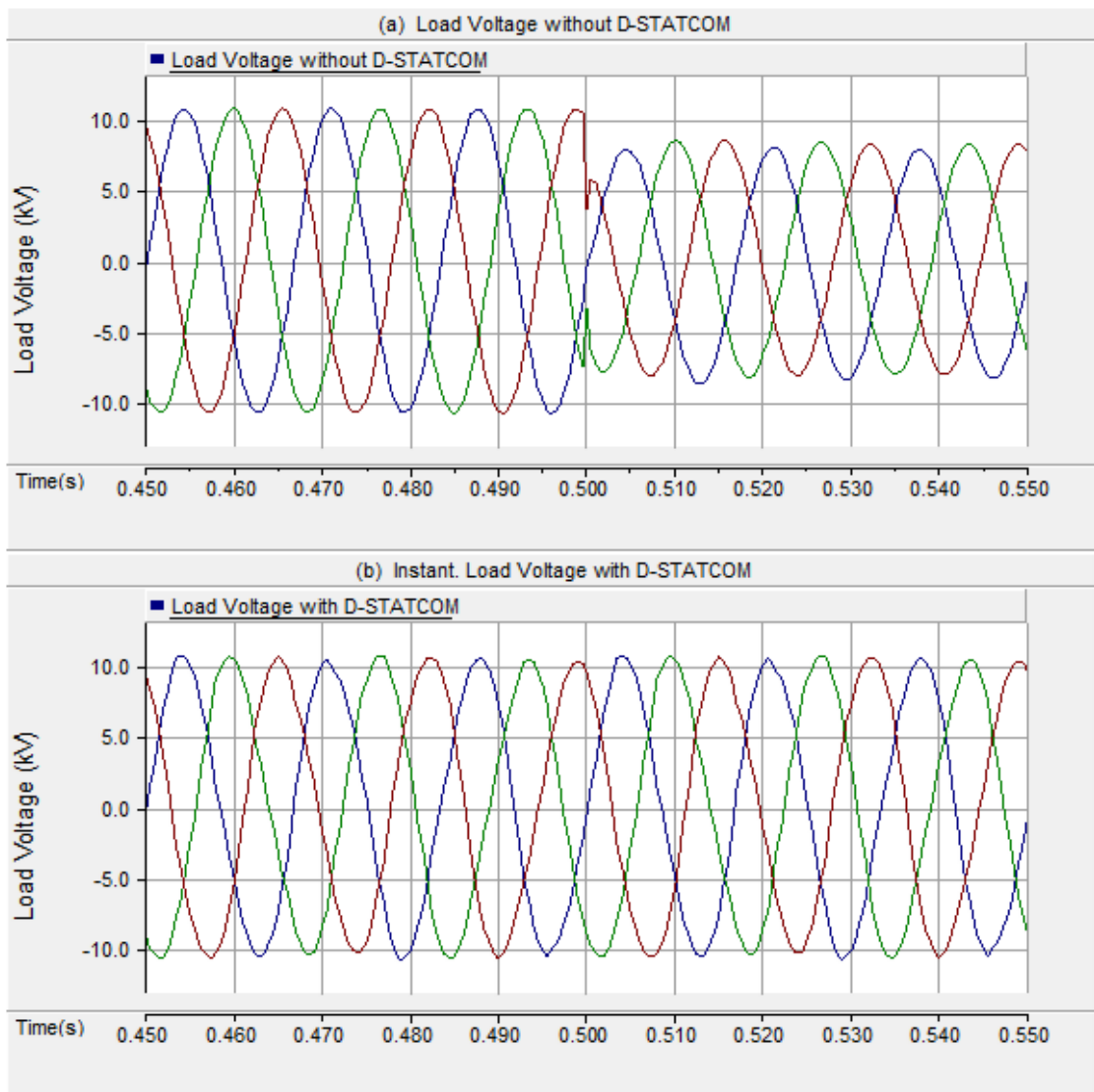
49

Fig. 4.4: Load voltage with and without D-STATCOM

The VSC generated these voltages by converting the DC voltage stored in the DC link capacitor using the required firing pulses obtained from PWM, to trigger the IGBTs. Curious observation show that, IGBTs on the same leg (arm) like IGBT 1 and 4 or 3 and 6, are not switched either ON or OFF simultaneously as desired. This implies that their respective switching signals are exactly apposite of one another as shown below. Fig. 4.5 shows the pair of firing pulses of each arm of the VSC for clear comparison.
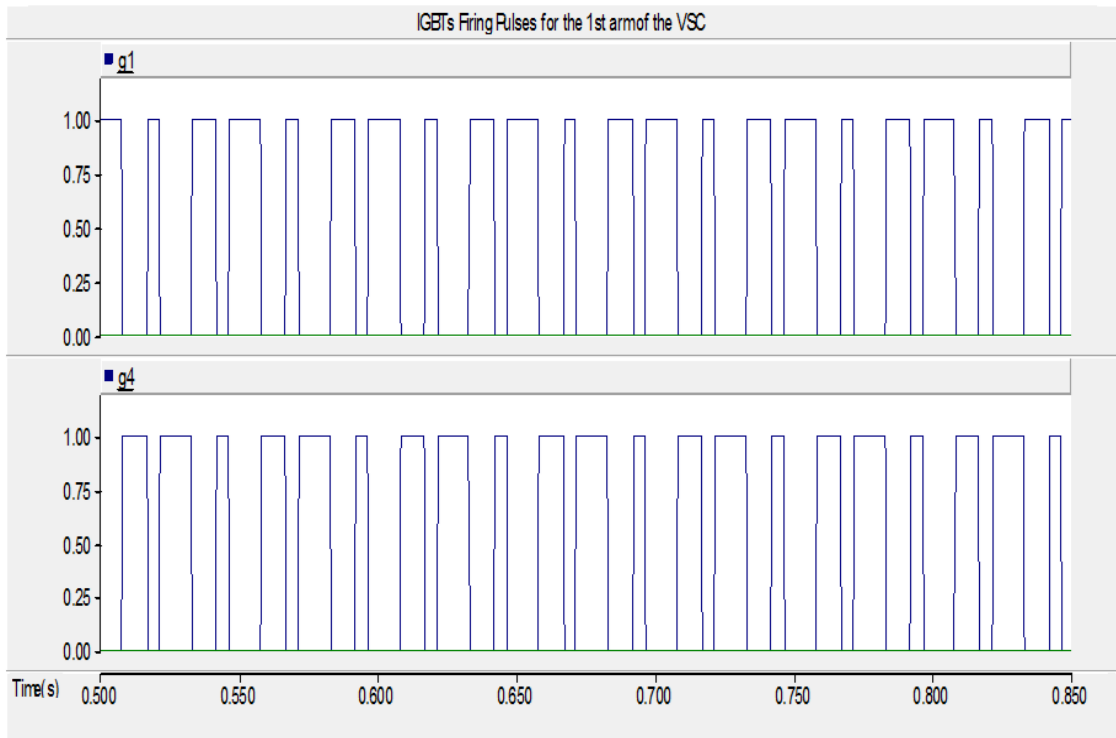
(a) Firing pulses for triggering the IGBTs on the first arm of the VSC (IGBT 1 and 4)
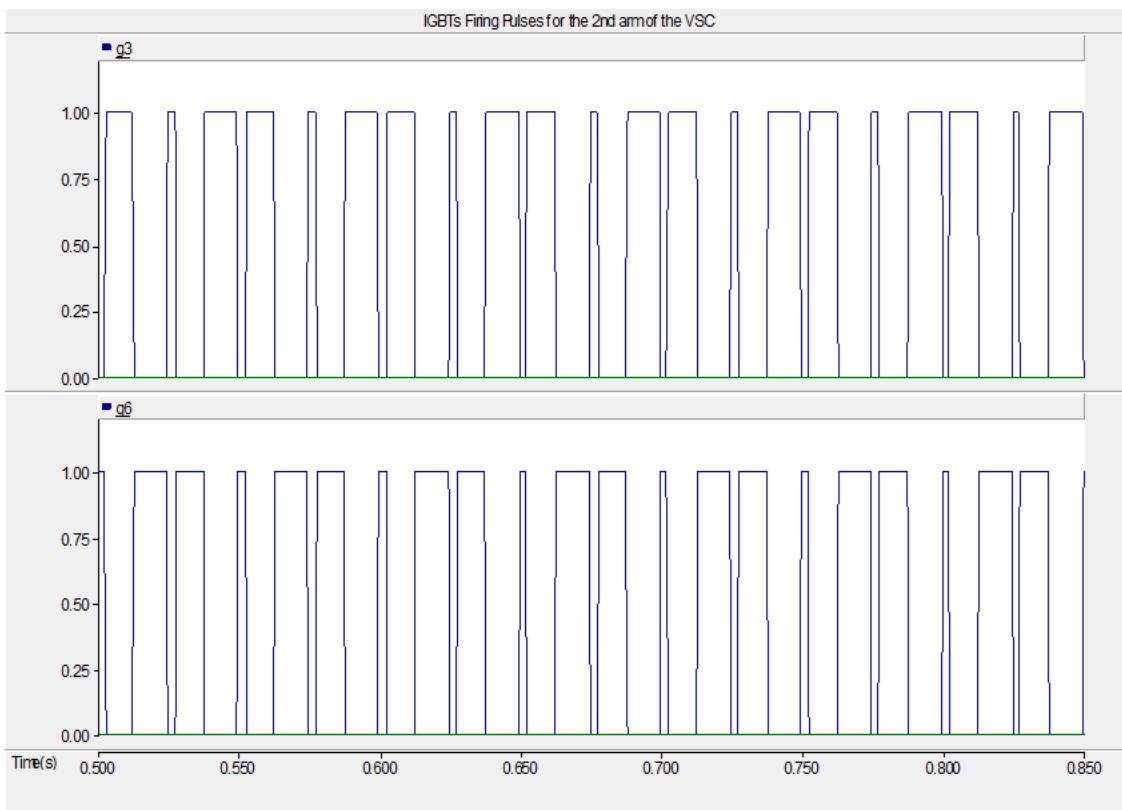
(b) Firing pulses for triggering the IGBTs on the first arm of the VSC (IGBT 3 and 6)
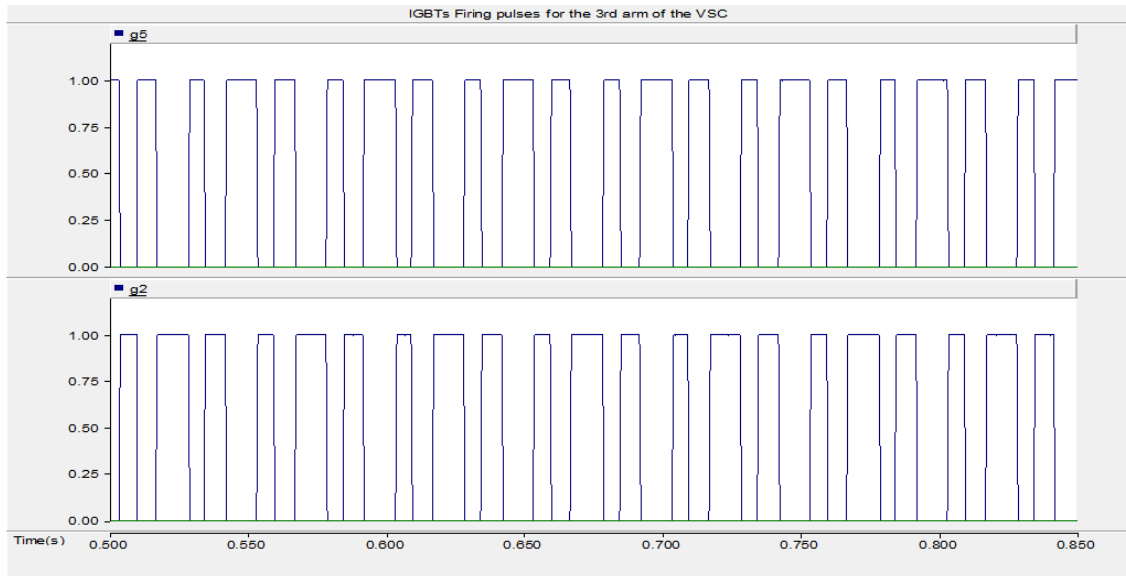
(c) Firing pulses for triggering the IGBTs on the first arm of the VSC (IGBT 5 and 2)

Fig. 4.5: PWM gate switching signals of the IGBTs

Consequent to the power exchange between the D-STATCOM and the AC system, the voltage across the DC link capacitor is not constant, as it continually been changing magnitude to achieve shunt compensation in order to keep the load voltage constant. Fig. 4.6 shows the DC link voltage variation during this shunt compensation.
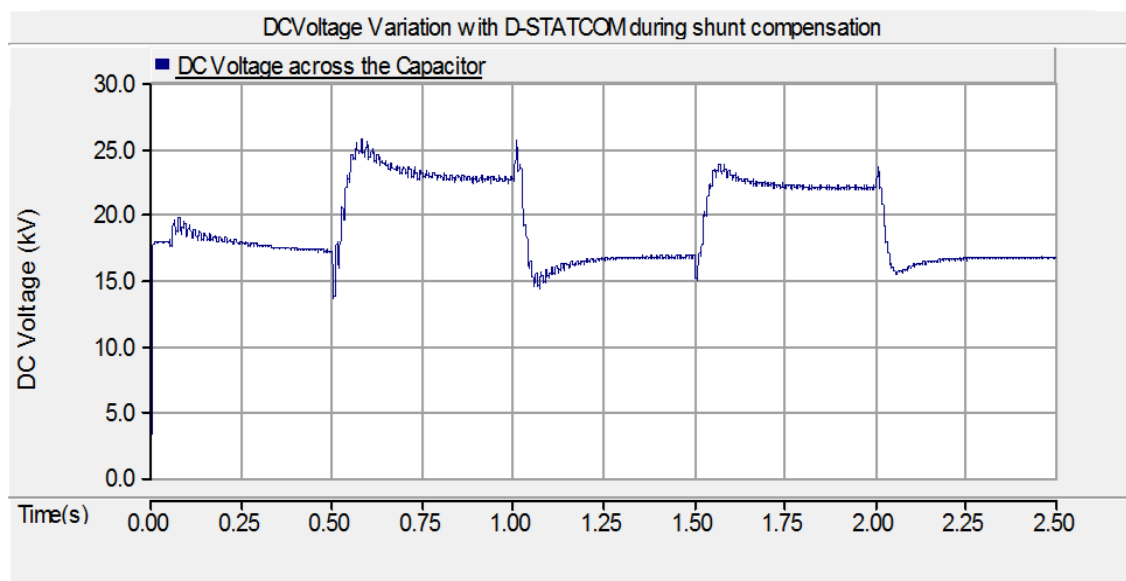

Fig. 4.6: DC Voltage with the D-STATCOM connected

4.1.2 Voltage Swell Mitigation Using D-STATCOM

To test the D-STATCOM's ability to alleviate voltage swelling, similar test system presented in Fig 4.1 of section 4.1.1, is used. However, in this case, the load is replaced with a load of $1.2MW - j2.25MVAR$ with a leading power of 0.65 as shown in Fig. 4.7, to create a three phase balanced voltage swell. The fault is also remove as it has been demonstrated above.

P+jQ
1.2 [MW] /ph
-2.25 [MVAR] /ph

Fig. 4.7: Sensitive Load PSCAD model with leading power factor
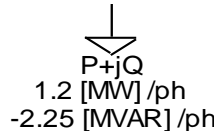
Similarly, the system is primarily tested without the D-STATCOM and later introduced. The sensitive load connected within the simulation period of $0.75 \leq t_s \leq$ 1.75sec has exerted a capacitive sensitive load effect on the system voltage thereby causing it to increase to virtually 21% as shown in Fig. 4.8.
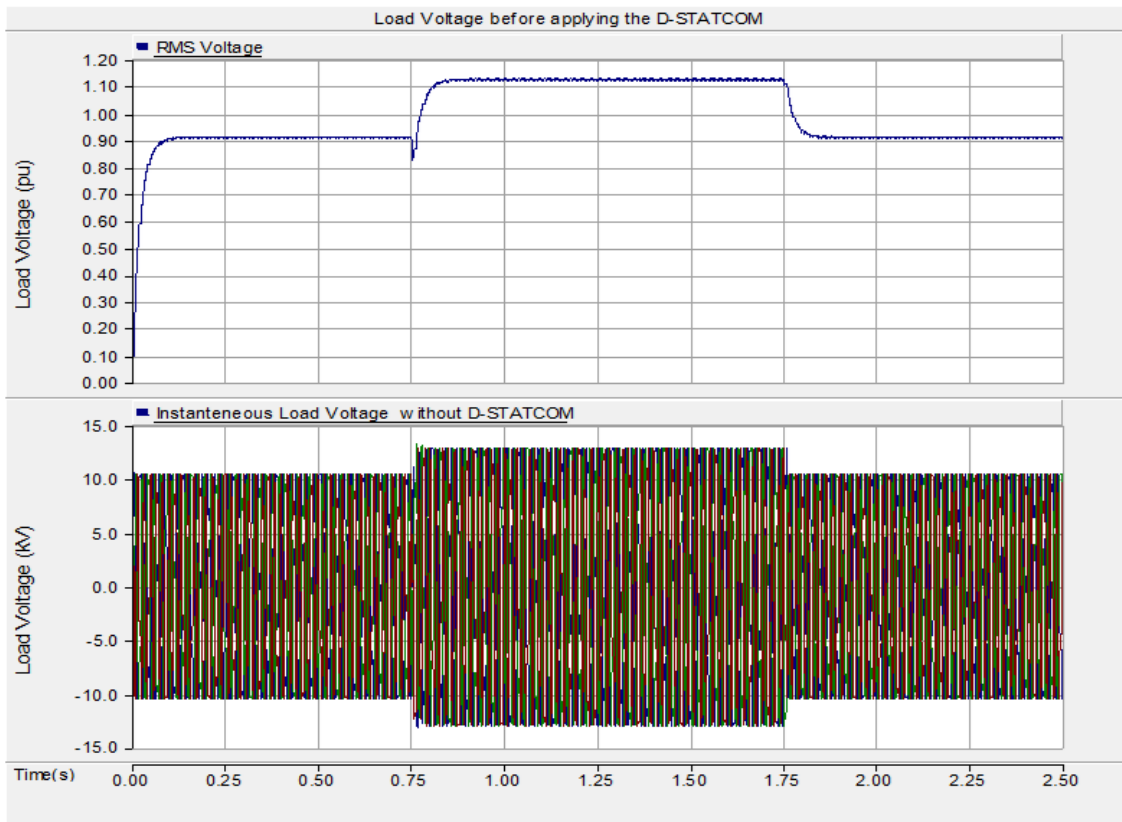
Fig. 4.8: Load Voltage before applying the D-STATCOM

Later, the D-STATCOM is introduced and the system is tested for the second time to ascertain its effectiveness. The device absorbed the reactive power and mitigate the voltage swell, in so doing, restored the load voltage to its nominal voltage of 1.0 p.u level as shown in Fig. 4.9 and summarized in Table 4.3.
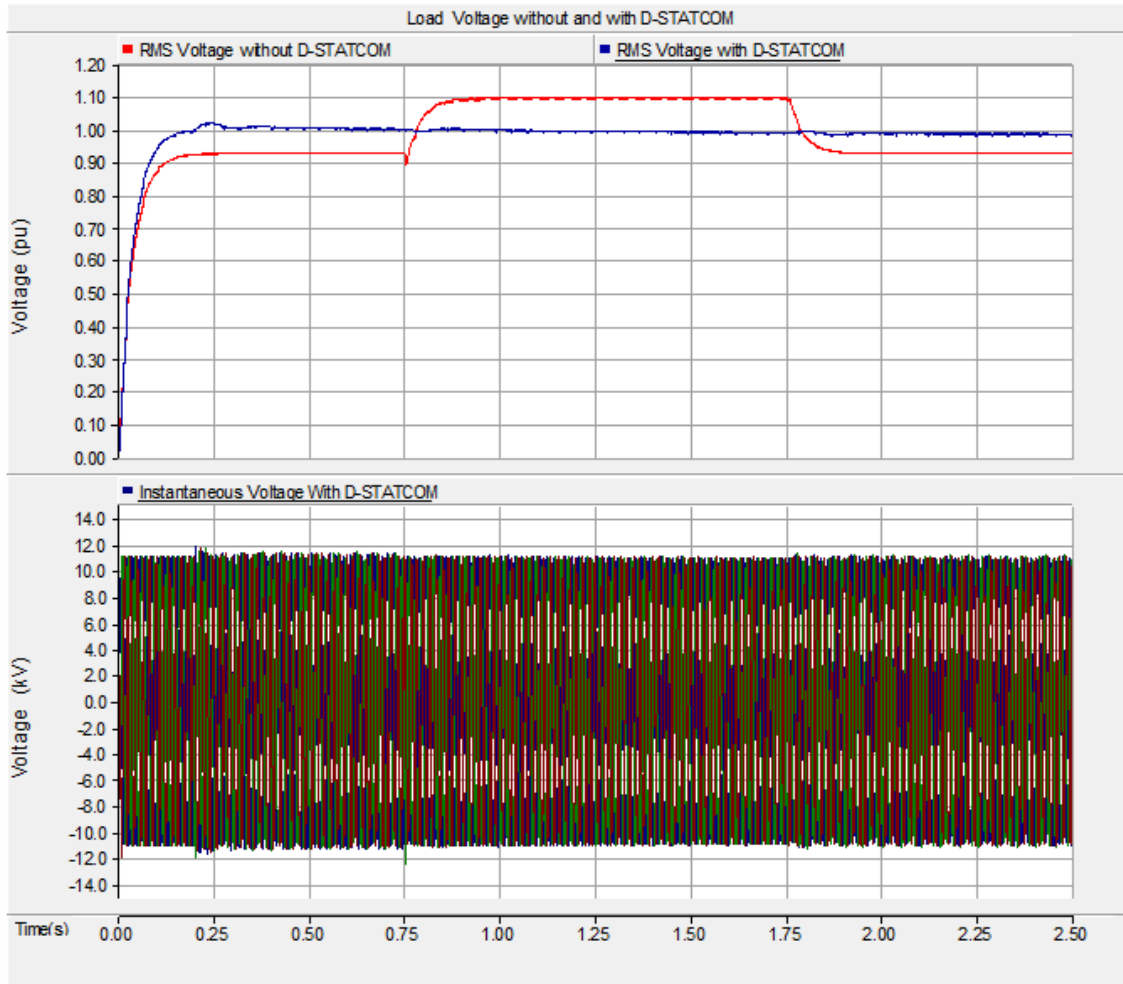
Fig. 4.9: Load voltage after the D-STATCOM has been applied

Table 4.3: Summary of voltage swell alleviation using D-STATCOM

Parameter	Simulation Time (s)	Without D-STATCOM	With D-STATCOM
RMS Voltage load (pu)	Without voltage swell	0.923	0.998
	$0.75 \leq t_s \leq 1.75$	1.110	1.015
Instantaneous Load Voltage (kV)	Without voltage swell	10.153	10.978
	$0.75 \leq t_s \leq 1.75$	12.210	11.165

4.1.3 D-STATCOM Test for Power Quality on PSS

To ascertain the effectiveness of D-STATCOM in power quality control on Photovoltaic Solar System (as Distributed Generation source), the test distribution system illustrated in Fig. 4.10 is used.
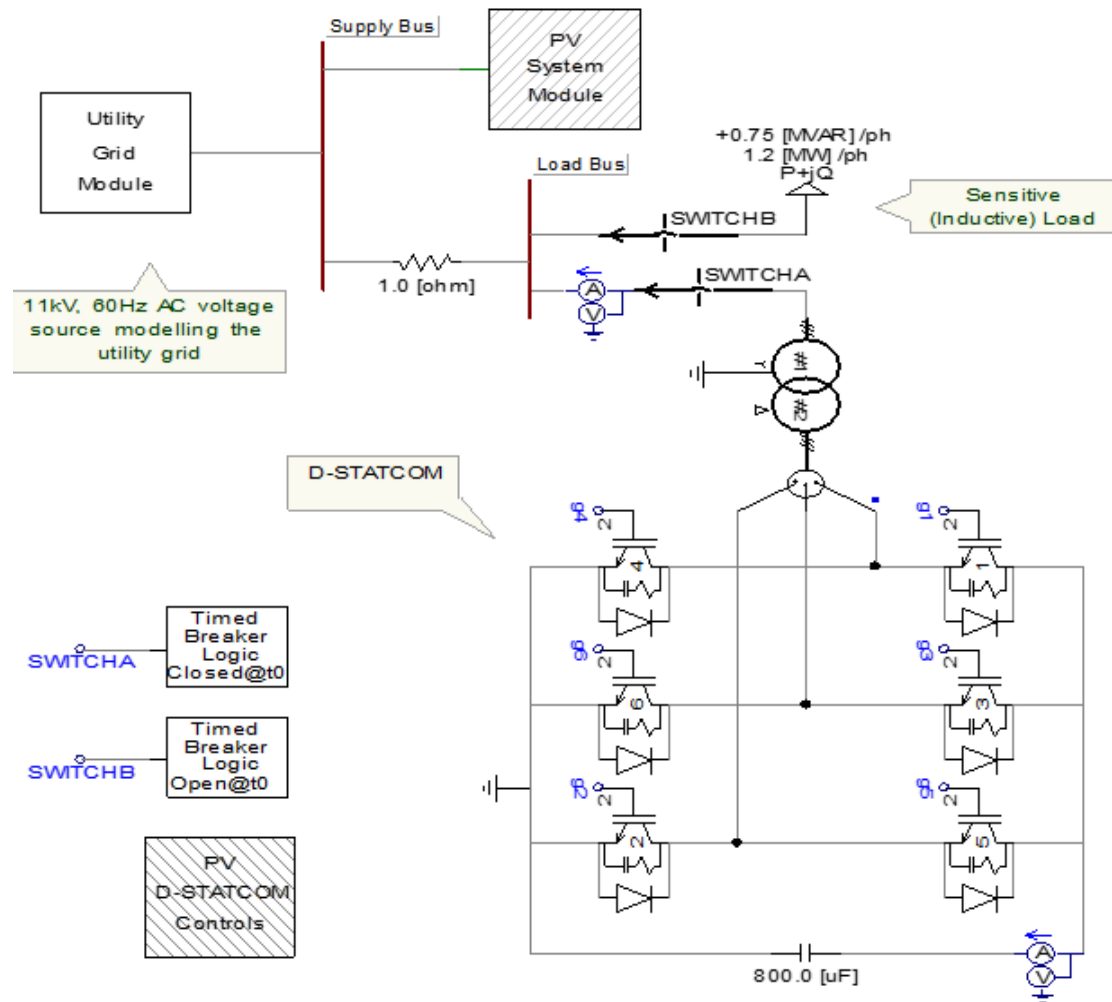
Fig. 4.10: D-STATCOM test system to improve PQ of PSS in PSCAD

Photovoltaic system's output depends largely on solar irradiation and temperature. Hence the simulation is carried out at Standard Test Conditions (STC) in which the system is tested under the irradiance intensity of 1000 W/m^2, AM1.5 solar reference spectrum and a cell temperature of 298K (25°C) which is expected to generate 1.0 MW on 270kV voltage level. With aid of the 270V/11kV, the voltage is stepped up to the system's nominal voltage of 11kV.

The system is tested to establish the PSS support to the DC link capacitor and hence the real and reactive power exchange before, during and after the dip. Fig 4.11 shows the voltage across the DC link capacitor with and without PV Support.

Fig. 4.11: Voltage across the DC link Capacitor with and without PV Support

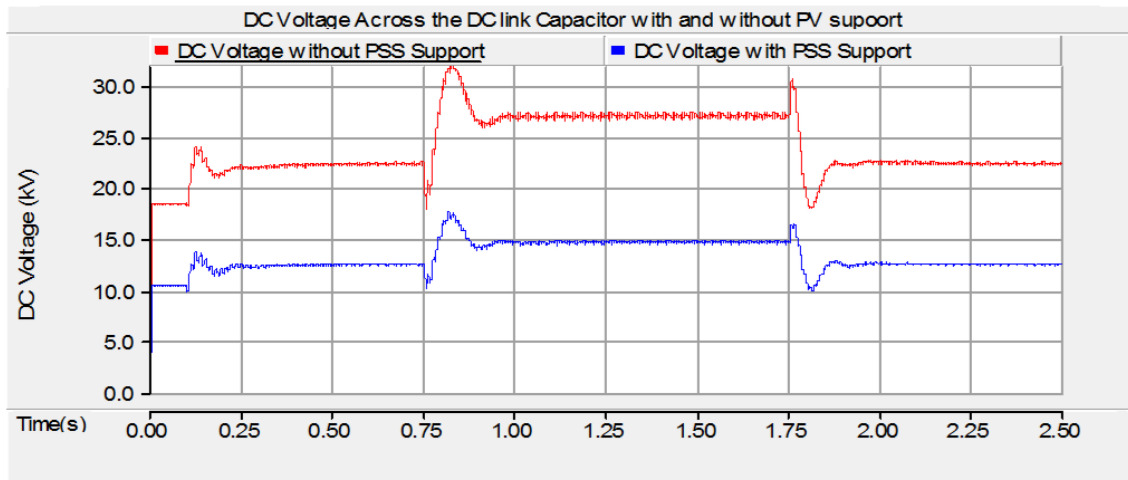Supporting the DC link capacitor has enormous consequence on the real and reactive power exchange between the D-STATCOM and the system. This is depicted in Fig. 4.12.
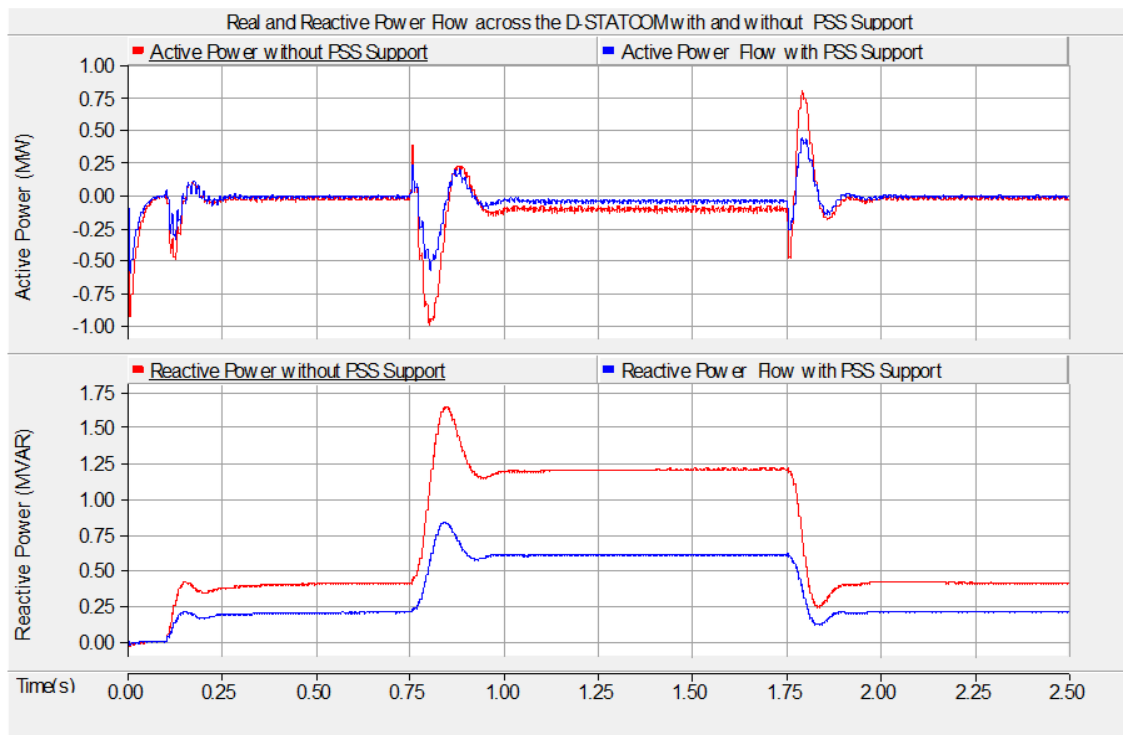

Fig. 4.12: Real and reactive power flow across the D-STATCOM with and without PSS

It can be deduced that installing PSS supports the DC link capacitor voltage by 9kV averagely, thereby reducing the active and reactive power exchanges between the D-STATCOM and the AC system by 260kW and 0.6MVA on average.

4.2 TESTS ON DVR

Similarly, three different tests are carried out on DVR to observe its usefulness in power quality control, namely:

➢ Voltage Sag Alleviation
➢ Voltage Swell Mitigation
➢ Grid-tied PSS Power Control

4.2.1 Voltage Sag Alleviation Using DVR

To test the DVR's ability in alleviating voltage dips, a test system comprising of 2-bus distribution system subjected to a three phase balanced fault is modeled. The timed three phase balanced fault shown in Fig. 4.13, caused the system's voltage to decrease thereby effecting its stability and that of the power quality.

(a)   Timed Fault Logic   (b) Balanced Fault   (c) Fault ON and OFF Resistances
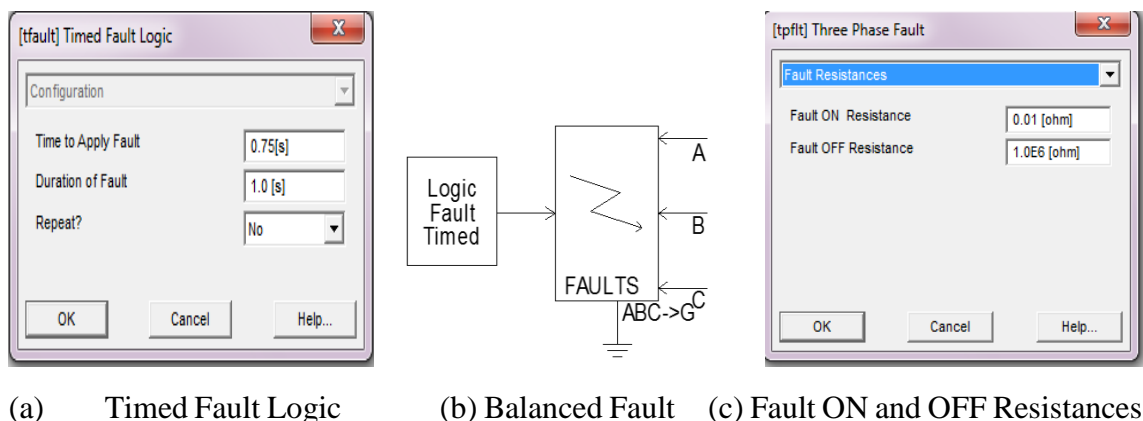
Fig. 4.13: Balanced Three Phase Fault with its Timing Control and Resistances

Fig. 4.14 shows the test system of the DVR with a total simulation period of 2.50 sec.
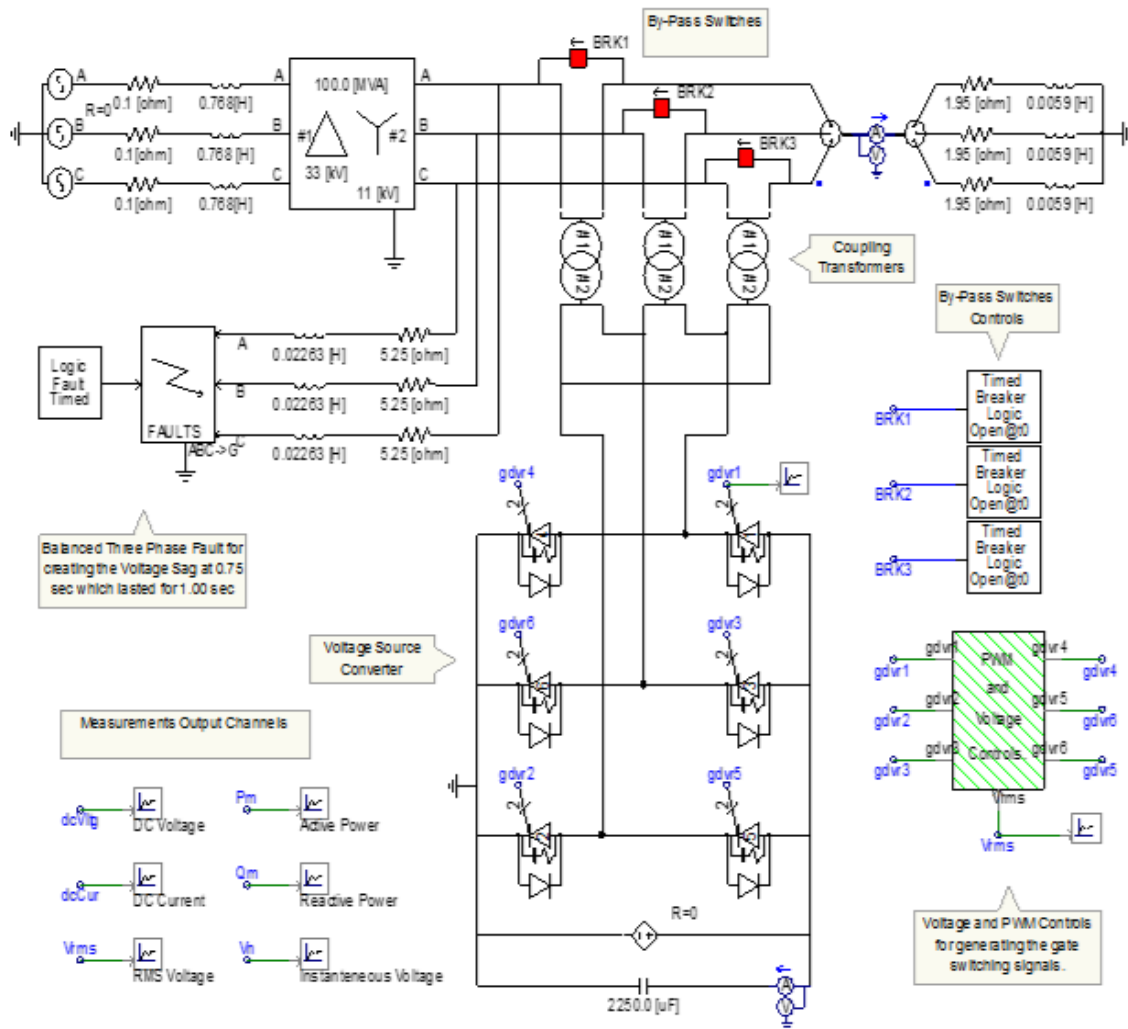
Fig. 4.14: Complete DVR Test System for Load Voltage Sag Protection

The Fault with very large ON and negligible OFF resistances of 1.0MΩ and 0.01Ω respectively, is switched ON with aid of Timed Control Logic at a simulation period, t_s of 0.75sec and lasted for additional 1.00 sec (0.75≤ t_s ≤1.75sec). This caused the voltage to decrease by roughly below 0.75pu of the system voltage as shown in Fig 4.15.
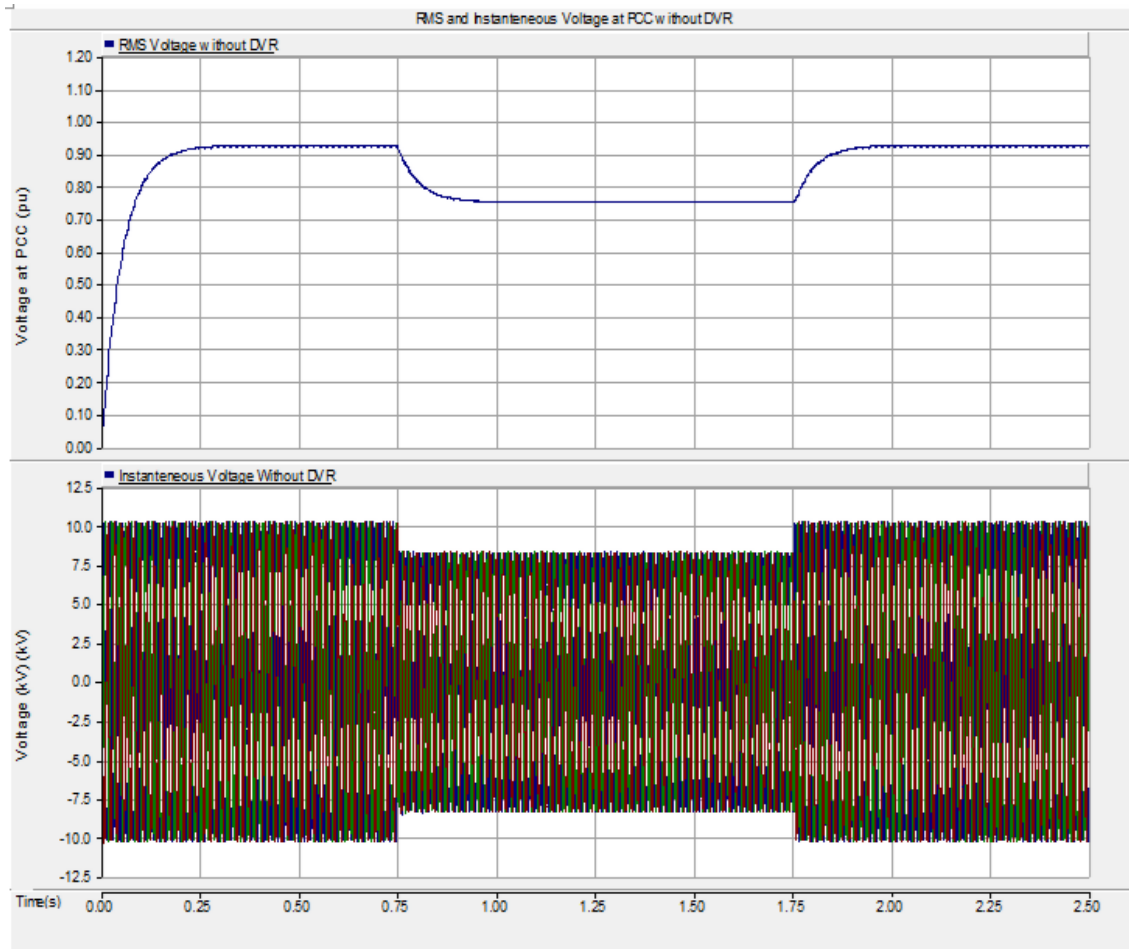
Fig. 4.15: RMS and instantaneous voltage without DVR under sagging effect

This has virtually similar effect of an inductive load, as it decreases the system voltage. The DVR is later connected via the coupling transformer which restores the system's voltage by injecting a voltage in series in phase with the load at the point of common coupling, PCC.
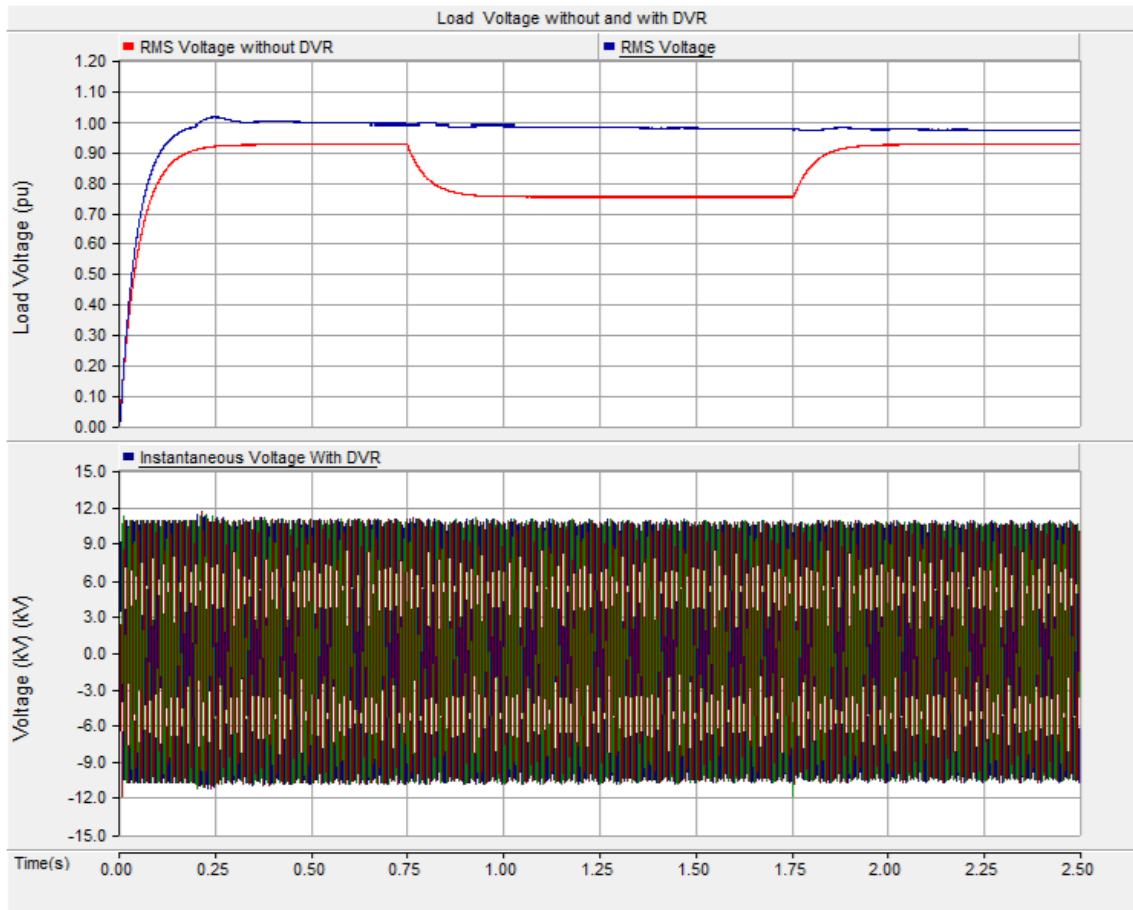
Fig 4.16 RMS and instantaneous voltage with and without DVR.

Because of the simulation time of 2.50sec and the frequency of the supply voltage, 60Hz, the waveform in Fig. 4.16 appear to be somehow clustered together. Hence, to clearly observe these waveforms, a close up view of the voltage before and after introducing the DVR within 6 periods is shown in Fig 4.17.
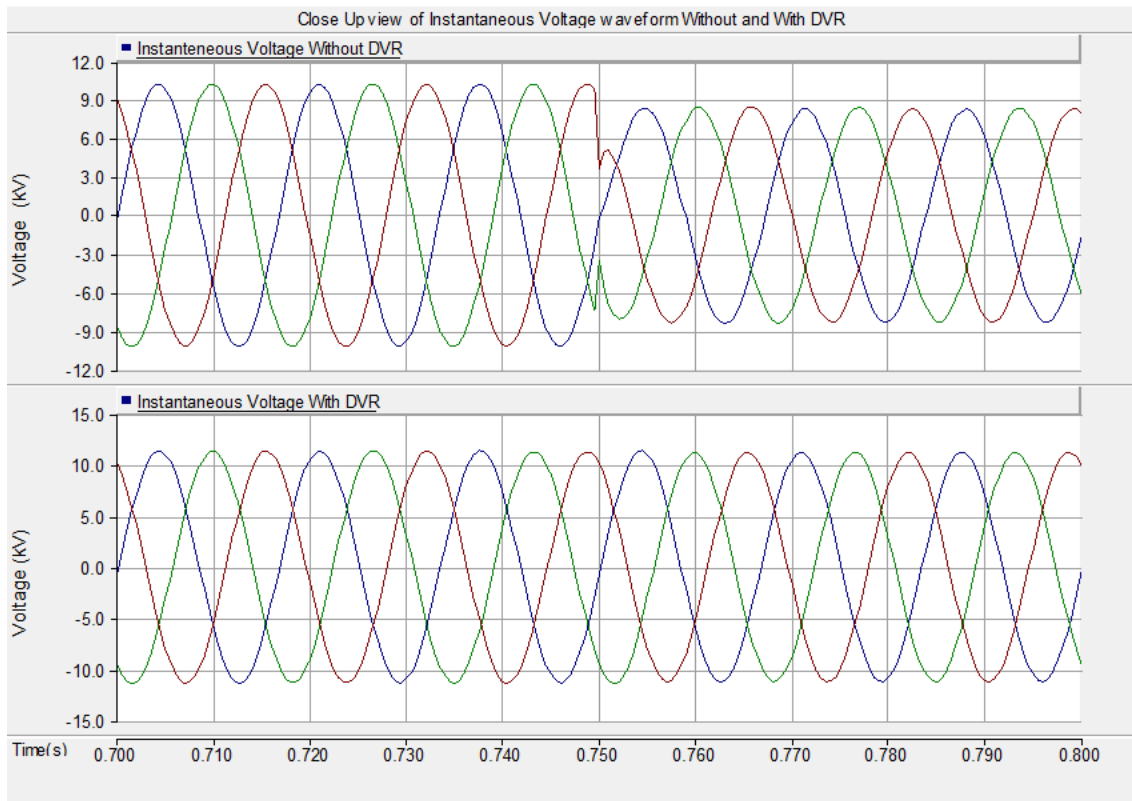
Fig. 4.17: Close up view of the voltage waveform without and with the DVR

These clearly demonstrate how capable DVR is, in mitigating voltage dips whenever there is fault or sudden connection of a sensitive inductive load. This is well within the acceptable 5% of the system voltage, as summarized in Table 4.4.

Table 4.4: Summary of voltage sag alleviation using DVR

| Parameter	Simulation Time (s)	Without DVR	With DVR
RMS Voltage load (pu)	Without voltage sag	0.942	0.992
	$0.75 \leq t_s \leq 1.75$	0.745	0.985
Instantaneous Load Voltage (kV)	Without voltage sag	10.175	10.912
	$0.75 \leq t_s \leq 1.75$	8.195	10.835

4.2.2 Voltage Swell Mitigation Using DVR

DVR plays an important role in mitigating voltage swell by injecting a series voltage which is 180^0 out of phase to the load voltage. In so doing, it suppress the

swelling in the load voltage and restore it to normal rated value of 1.0 per unit. To demonstrate this, a test system depicted in Fig 4.14 is used. However, the fault that causes the sag is replaced with a sensitive capacitive load of $1.05\ MW - j1.95\ MVAR$. The sudden connection of capacitive load causes the voltage to swell and effect the power quality henceforth unless the issue is brought under control. It caused the voltage to increase to more than 12% of the rated value as shown in Fig. 4.18.
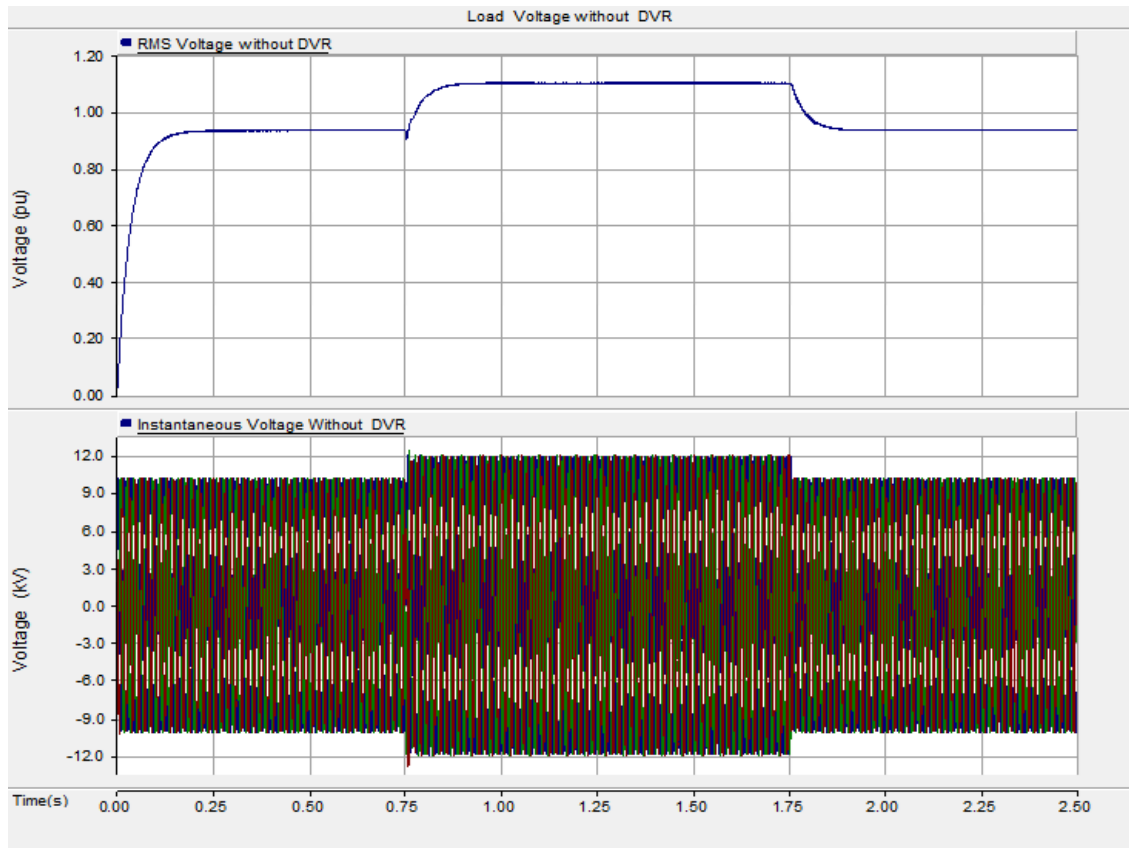
Fig. 4.18: RMS and instantaneous voltage without DVR under swelling effect

The system is simulated for a second time with the DVR connected with aid of the by-pass switches; BRK1, BRK2 and BRK3. The DVR injects a three phase series compensation voltage which is almost 180^0 out of phase to the load voltage in order to restore it to normality.
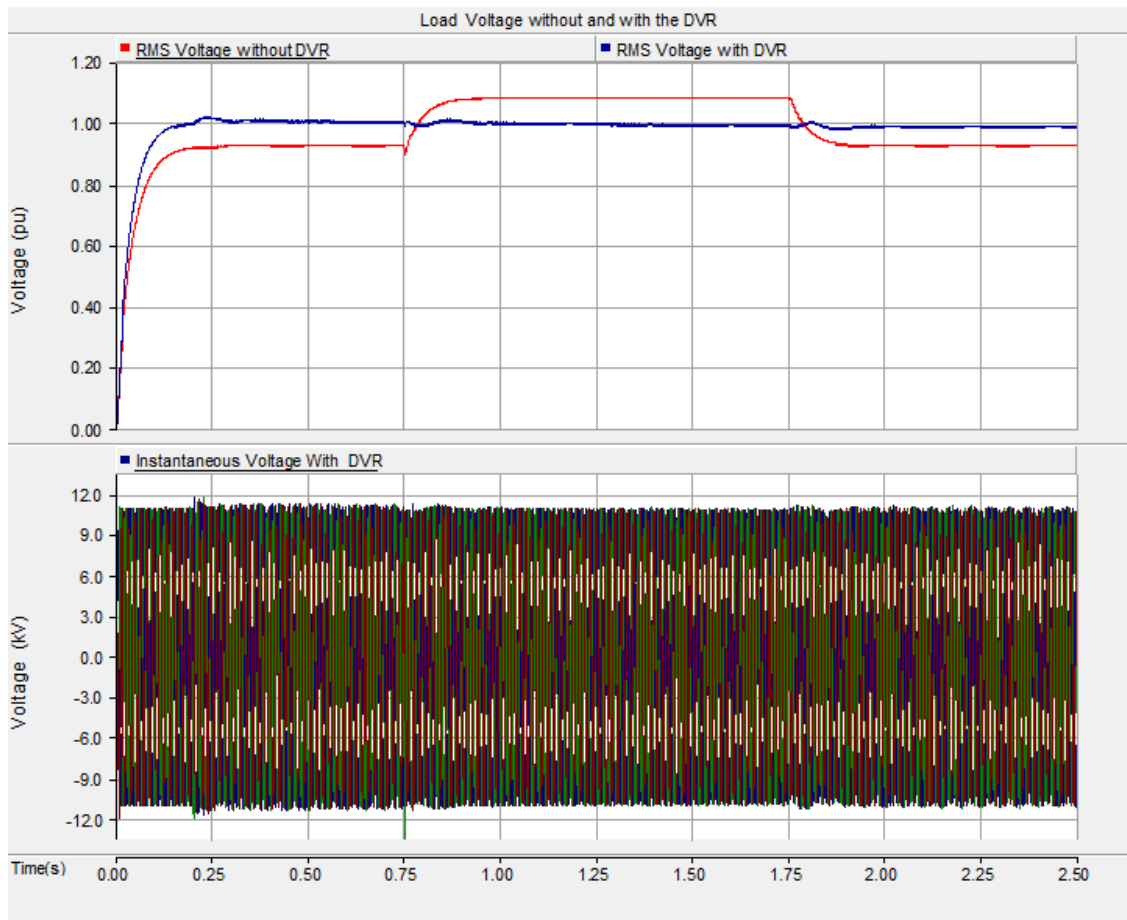
Fig. 4.19: RMS and instantaneous voltage with and without DVR under swelling effect

These visibly demonstrate DVR's ability in mitigating voltage swelling whenever there is a fault or sudden connection of the sensitive capacitive load. However, the quality of the power is slightly distorted due to the series reactance of the coupling transformer. This is summarized in Table 4.5.

Table 4.5: Summary of voltage swell mitigation using DVR

Parameter	Simulation Time (s)	Without DVR	With DVR
RMS Voltage load (pu)	Without voltage swell	0.935	0.995
	$0.75 \leq t_s \leq 1.75$	1.102	1.011
Instantaneous Load Voltage (kV)	Without voltage swell	10.935	10.945
	$0.75 \leq t_s \leq 1.75$	12.122	11.121

This series compensation is achieved through real and reactive power exchanges between the load and the DVR as described in section 2.3.4. Fig. 4.20 below shows the exchanges of real and reactive power while compensating the voltage swell.
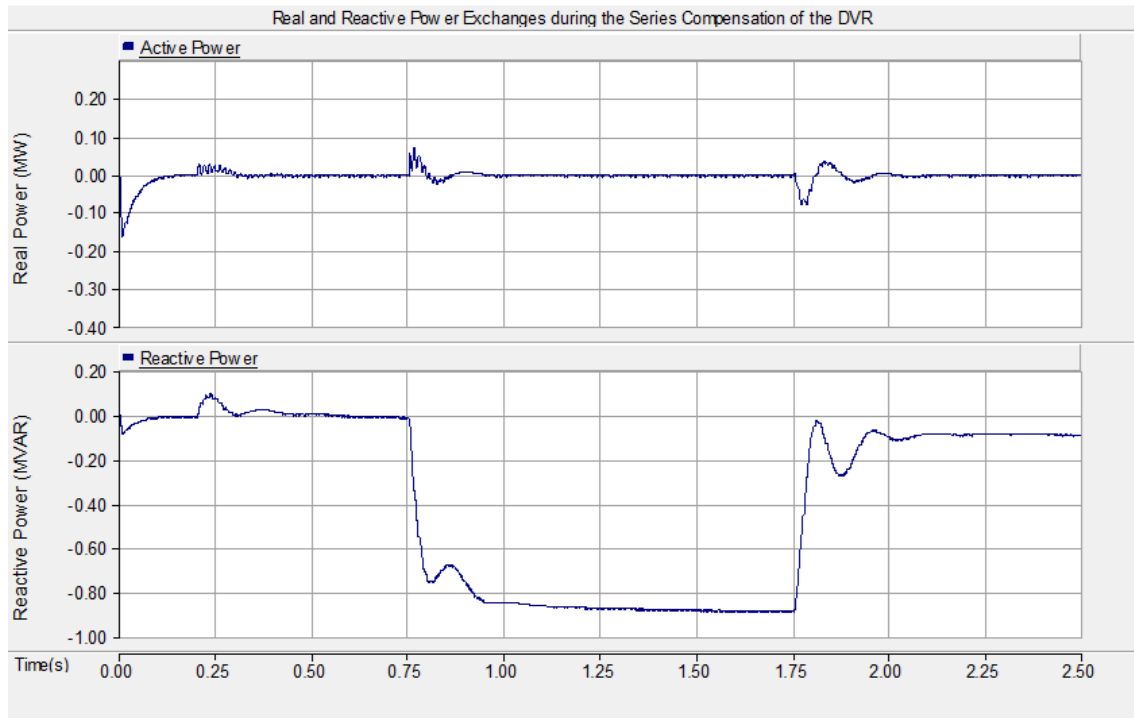
Fig. 4.20: Real and reactive power exchanges between the load and the DVR

4.2.3 DVR Test for Power Quality on PSS

Introducing PSS to the system increases the power handling capacity of the DVR, however distorting the quality of the voltage. But the DVR restores the voltage quality even if there is fault along the line as previously discussed. Fig. 4.21 shows the test system used to observe the PSS support to the DC link capacitor of the DVR, hence the real and reactive power flow to and from the system.

64
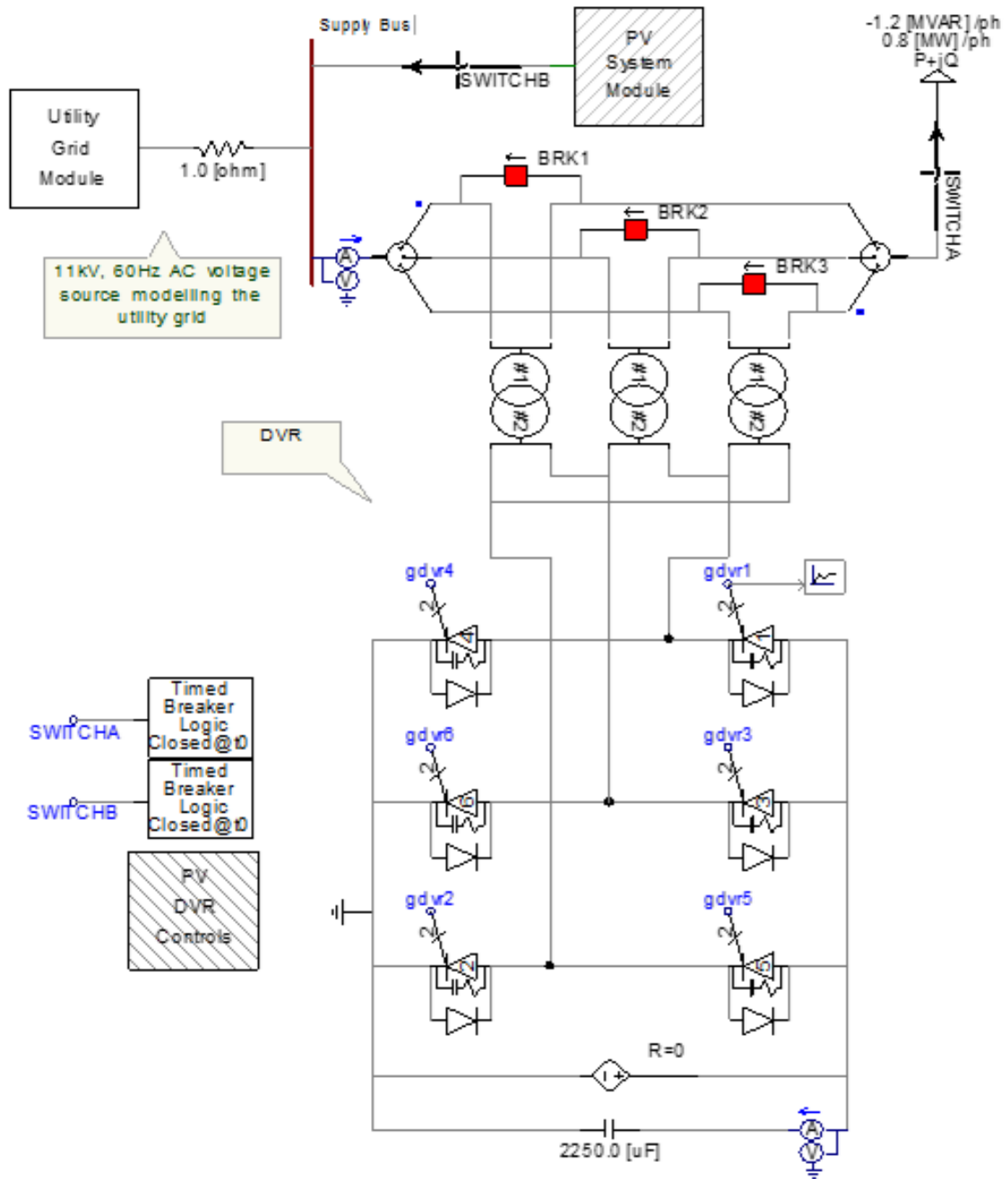
Fig. 4.21: DVR test system for integrating PSS to the Grid in PSCAD

The test system comprises of a grid module, a sensitive load of $0.8\ MW - j1.2\ MVA$, the PSS and the DVR with their respective controls. It is simulated first with the sensitive load connected within a simulation period of $0.75 \leq t_s \leq 1.75$sec whose effect is to increase the voltage at the PCC. The DVR alleviate this voltage instability as described in Section 4.2.2. However, the DC voltage across the DC link is siphoned out, hence PSS is introduced. The system is simulated for the second time, it has been observed that the DC voltage is improved by roughly 9.5kV from the PSS as shown in Fig. 4.22.

Fig. 4.22: DVR DC link voltage with and without PSS support

Integrating the PSS do not only support the DC link, but improve the real and reactive power flow between the DVR and the AC system as shown in Fig. 4.23.

Fig. 4.23: Active and reactive power flow across the DVR with and without PSS

It can be deduced that introducing the PSS improved the active and reactive power flow by 450kV and 720kVA respectively.

66

CHAPTER FIVE

CONCLUSION AND RECOMMENDATIONS.

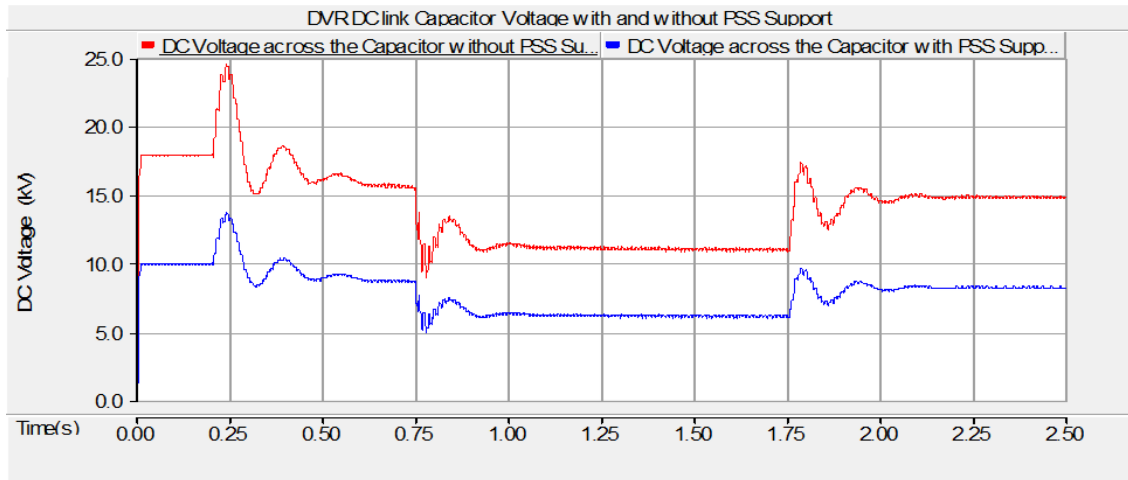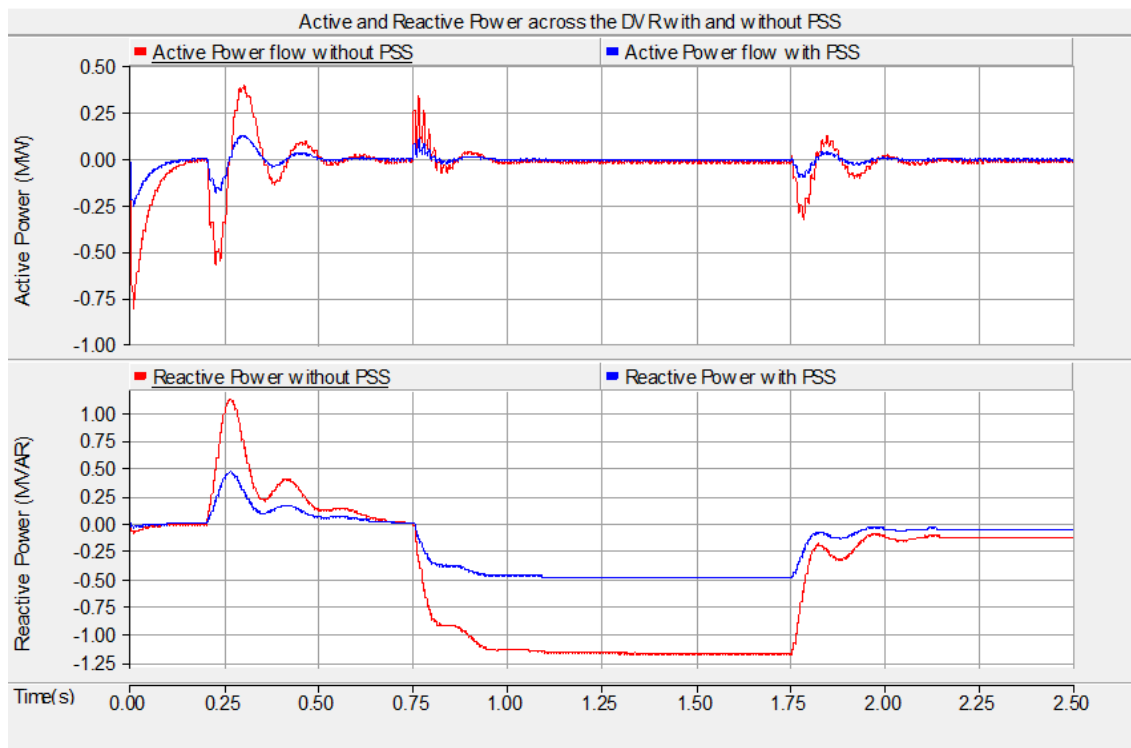The present power system need a state-of-the-art transformation due to the sudden hike in demand of the electrical power. Smart Grid is presented as a solution to almost all the problems in power systems, as all aspect of the system is improved ranging from generation, transmission, distribution, utilization and communication systems.

To achieve this state-of-the-art system, be it on Transmission or Distribution level, power electronic devices are of great and inevitable importance due to the fast-solid-state switching devices driven by modern control algorithms used. They are employed for power quality applications, enhancing two-way power flow and coupling DGs to the grid among others.

Among these devices used in the distribution system (called Custom Power Devices), D-STATCOM and DVR have shown significant performance especially for voltage stability, integrating DGS, active and reactive power compensation. The PWM-based control implemented to control the valves of the IGBTs of the VSC used in this thesis is among the best if not the best. They are modeled and simulated to demonstrate their capabilities in mitigating voltage instability and integrating disperse generation sources.

It has been established from the results obtained that DSTATCOM mitigated voltage dips and restores the system voltage much better than the DVR. However, DVR alleviates voltage swell much better than D-STATCOM. This is due to the shunt compensation whose coupling transformer's reactance exert less effect on the system voltage. In fact, it has been helpful in filtering some ripples and suppressing some harmonics. This is why filter design for the D-STATCOM and DVR is not included within the scope of this thesis.

Moreover, it can be deduced from the tests carried out when the PSS is connected that, integrating DGs in to utility grid improves the power and the voltage, however distorting its quality. With aid of power electronic devices, these distortions can be corrected.

FUTURE WORK:

Many contributions are needed to change the entire conventional grid into Smart Gird. These includes data acquisition, communication, automation and improving the generation, transmission and distribution system of the network. It is should be, as part of future work of this thesis, to include data acquisition and communication gadgets in the presented networks. Then transient stability, harmonics distortions studies and power flow analysis should be carried out.

Modeling of more sophisticated devices like Back-to-back STATCOM and UPFC, more DGs facilities like wind farms, fuel cell will also be part of the future plan of the thesis.

REFERENCES

[1] Q. Fu, L. F. Montoya, A. Solanki, A. Nasiri, V. Bhavaraju, T. Abdullah and D.C Yu, "Microgrid Generation Capacity Design with Renewables and Energy Storage Addressing Power Quality and Surety", *IEEE Transaction on Smart Grid,* Vol.3, No. 4, pp. 2019-2027, December 2012.

[2] P. Kundur, *Power System Stability and Control,* McGraw-Hill, Newyork, 1993.

[3] S. Kazemi, *Reliability Evaluation of Smart Distribution Grid*, Ph.D Dissertation, Aalto University, 2011.

[4] A. M. Vural, *Modelling of Multi-Converter FACTs (Flexible Alternating Current Transmission Sytstems)*, PhD Dissertation, Cukurova University, 2012.

[5] A. K. Mohanty and A. K. Barik, "Power System Stability Improvement using FACTs Devices", *International Journal of Modern Engineering Research (IJMER),* Vol. 1, Issue-2, pp. 666-672.

[6] M. Gomez, O. Abarrategui and I. Zamora, *FACTs Devices in Distributed generation,* University of the Basque Country, 2010.

[7] H. Gharavi and R. Ghafurain, " Smart Grid: The Electric System of the Future", *Proceedings of the IEEE,* Vol. 99, No. 6, pp. 917-921, June 2004.

[8]   F. Blaabjerg, Z. Chen and S. B. Kjaer, " Power Electronics as Efficient Interface in Disperse Power Generation Systems," *IEEE Transaction on Power Electronics,* Vol. 19, No. 5, pp. 1184-1194, September 2004.

[9]   J. Kim, S. Cho and H. Shin, " Advanced Power Distribution System Configuration for Smart Grid", *IEEE Transactions on Smart Grid,* Vol. 4, No. 1, March 2013.

[10] O. Gulich, *Technological and Business Challenges of Smart Grid*, M. S. Thesis, Lappeenranta University of Technology, 2010.

[11] S. Balani, *Smart Grid Technologies for Efficiency Improvement of Integrated Industrial Electric System,* PhD Dissertation, University of New Orleans, 2011.

[12] E.E.C Moraes, S. J. deMesquita, R. P. S Leao, M.B.M Neto and L. C. Leite, "The Application of D-STATCOM in Smart Distribution Grid with Wind Power Plants", *IEEE Transaction on Industry Application,* Vol. 7, No. 5, pp. 1-6, November 2012.

[13] M. P. Donsion, J. A. Guemes, J. M. Rodriguez "Power Quality Benefits of Utilizing FACTS Devices in Electrical Power System", *International Journal of Electronics and Communications (IJECs)*, Vol. 1, Issue-1, pp. 47-52, August 2012.

[14] E. Acha, B. G Agelidis, O. Anaya-Lara and T.J.E Miller, *Power Electronics Control in Electrical System,* Newnes, Butterworth, Linacre House, Jordan Hill, Oxford, 2000.

[15] M. Malla, N. Pradhan, N. B. Araya and T. A. Adamu, *Power Quality Improvement in Smart Distribution Grids Using Power Electronics Converters*, Mini-report in Power Electronics for Renewable Energy, TET4190, Norwegian University of Science and Technology, 2010.

[16] R. Resmi, V. Reshmi and J. Jacob, " Mitigation of Voltage Sag, Swell and Harmonics by Dynamic Voltage Restorer using Matrix Converter," *International Journal of Advanced Researchin Electrical, Electronics and Instrumentation Engineering,* Vol. 2, Special Issue-2, pp. 297-304, December 2013.

[17] B. Kanchanpalli and M.Valavala, "Implementation of Custom Power Device in PSCAD/EMTDC for Power Quality Improvement", *International Journal of Electronics and Communications (IJECs)*, Vol. 1, Issue-1, pp. 47-52, August 2012.

[18] T. D. Haskell, *Modelling and Analysis of a Dynamic Voltage Regulator*, M. S. Thesis, California State University, 2013.

[19] U.S Department of Energy, *"Benefits of Using Mobile Transformers and Mobile Substation for Rapidly Restoring Electrical Service*: A Report to the United States Congress Pursuant to Section 1816 of the Energy Policy Act of 2005", 2006.

[20] Hitachi, *We Support the Next Generation Energy Networks, for the Earth, 2014,* http://www.hitachi.com/environment/showcase/solution/energy/smartgrid.html

[21] Pilih Bahasa, *Renewable and Non-renewable Energy Sources, 2013.* http://independent.cc.web.id/ lain.php? en=ENGLISH& lain=21260

[22] Y. K. Abdulrahman, " PSCAD Simulation of Grid-Tied Photovoltaics Systems and Total Harmonics Distortion Analysis", *International Journal on Electrical Power and Energy Conversion Systems,* Vol. 4, No. 2, pp. 1-6, October 2013.

[23] S. A. Rahman and R. K. Varma, "PSCAD/EMTDC Model of a 3-Phase Grid Connected Phtovoltaic Solar System", *North American Power System Symposium (NAPs)*, Vol. 6, No.4, pp. 1-7, August 2011.

[24] B. A. Johnson, *Modelling of a PV Grid-Tied Smart Inverter's Support Function,* M. S. Thesis, California State University, 2013.

[25] IEEE, *Standard Dictionary of Electrical and Electronic Terms, 6ᵗʰ edition,* IEEE Std 100-1996, March 2012.

[26] P. Ananthababu, B. Trinadha and K. Ramcharan, "Performance of Dynamic Voltage Restorer (DVR) against Voltage Sags and Swells using Space Vector PWM Technique", *International Conference on Advances in Computing, Control and Telecommunication Technologies,* Vol. 28, No. 4, pp. 206-210, December 2009.

[27] H. P. Tiwari and S. K. Gupta, "DC Energy Storage Schemes for DVR Voltage Sag Mitigation System", *International Journal Computer Theory and Engineering,* Vol. 2, No. 3, pp. 1793-8201, June 2010.

[28] H. P. Tiwari and S. K. Gupta, "DVR based on Fuel Cell: An Innovative Back-up System", *International Journal of Environmental Science and Development,* Vol. 1, No.1, pp. 73-78, April 2010.

[29] J. G. Nielsen and F. Blaabjerg, "A Detailed Comparison of System Topologies for Dynamic Voltage Restorers", *IEEE Transactions on Industry Application,* Vol. 41, No. 5, pp. 1272-1280, September 2005.

[30] A. Helal, S. Z. Elabideen and A. Lofty, "Modelling and Analysis of SVPWM Based Dynamic Voltage Restorer", *World Academy of Science, Engineering and Technology,* Vol. 48, No.29, pp. 151-156, December 2010.